Variations in Architecture and Cyclicity in Fault-bounded Carbonate Platforms: Early Miocene Red Sea Rift, NW Saudi Arabia

Ardiansyah Koeshidayatullah[1], Khalid Al-Ramadan[1], Richard Collier[2], Geraint Wyn Hughes[1,3]

[1]Earth Sciences Department, King Fahd University of Petroleum and Minerals, Dhahran, Saudi Arabia, 31261

[2]Basin Structure Group, School of Earth and Environment, University of Leeds, LS2 9JT, UK

[3]Applied Microfacies Ltd, Denbigh, UK

Corresponding author:

ardiansyah.ik@gmail.com

Dhahran, Saudi Arabia,

P.O Box 31261

ABSTRACT

The Early Miocene was a period of active rifting and carbonate platform development in the Midyan Peninsula, NW Saudi Arabia. However, there is no published literatures available dealing with detail characterization of the different carbonate platforms in this study area. Therefore, this study aims at presenting new stratigraphic architectural models that illustrate the formation of different carbonate platforms in the region and its forcing mechanisms that likely drove their formation. This study identified the following features formed during active rifting: a) a Late Aquitanian (N4) fault-block hangingwall dipslope carbonate ramp b) a Late Burdigalian (N7-N8) isolated normal fault-controlled carbonate platform with associated slope deposits, and c) a Late Burdigalian (N7-N8) attached fault-bounded, rimmed shelf developed on a footwall fault-tip within a basin margin structural relay zone formed coinciding with the second stage of rifting. Variations in cyclicity have been observed within the internal stratigraphic architecture of each platform and also between platforms. High-resolution sequence stratigraphic analysis show parasequences observed as the smallest depositional packages (meter-scale cycles) within the platforms. The hangingwall dipslope carbonate ramp and the attached platform demonstrate aggradational-progradational parasequence stacking patterns. These locations appear to have been more sensitive to eustatic cyclicities, despite the active tectonic setting. The isolated, fault-controlled carbonate platform reveals disorganized stratal geometries in both platform-top and slope facies, suggesting a more complex interplay of rates of tectonic uplift and subsidence, variation in carbonate productivity, and resedimentation of carbonates, such that any sea-level cyclicity is obscure. This study explores the interplay between different forcing mechanisms in the evolution of carbonate platforms in active extensional tectonic regions. Characterization of detailed parasequence-scale internal architecture allows the spatial variation in syn-depositional relative base-level changes to be inferred and is critical for understanding the development of rift basin carbonate platforms.

Such concepts may be useful for the prediction of subsurface facies relationships beyond interwell areas in hydrocarbon exploration and reservoir modeling activities.

Keywords: Red Sea, syn-rift, carbonate platform, stratigraphic architecture, parasequence stacking

1. INTRODUCTION

The sedimentology and stratigraphy of carbonate platforms provide useful information to delineate the evolution of marine basins (i.e. Tucker, 1985), and the prevailing palaeoenvironmental conditions at the time of deposition, including seawater chemistry and biological affinities (James, 1983; Schlager 1992; Gomez-Perez et al., 1999; Schlager, 2005). Three major controls have been proposed to account for the development and evolution of carbonate platforms in rift settings:

(i) Tectonic activity: Subsidence and footwall uplift caused by tectonic activity may create or reduce accommodation space for the accumulation of carbonate sediments, provide topographic areas for carbonate producers to nucleate or terminate carbonate productivity by drowning, and control the evolution of the carbonate platform geometry (Leeder and Gawthorpe, 1987; Gawthorpe and Leeder, 2000; Bosence, 2005; Mack et al., 2009). The concept of tectonic control on the stratigraphic evolution of clastic strata in syn-rift settings has recently been applied to carbonate deposition, through the development of depositional models and the interpretation of successions within syn-rift tectonic settings (Dorobek, 2008; Cross and Bosence, 2008; Merino-Tome et al., 2012). (ii) Relative variations in sea level: Sea level fluctuations play a major role in determining the extent of accommodation space created, and together with physiography of the substrate, these may govern the capacity for carbonate sediment production by light-dependent producers, such as corals, algae, and other heterotrophic organisms with carbonate skeletons and photosymbionts (Kendall and Schlager, 1981; Strasser et al., 1999; Pomar and Kendall, 2008; Bover-Arnal et al., 2009). Trends in relative sea level fluctuations can be identified by the presence and nature of several biofacies. Dorobek (2008) and Cross & Bosence (2008) have explored the interaction of lateral variations in tectonic displacement rates with eustatic variations in determining local variations in relative base level change in fault-bounded platform settings. (iii) Ecological accommodation: This third factor, the presence of carbonate-producing biota associated with particular hydrodynamic levels and other ecological factors, distinguish carbonate systems from siliciclastic systems (Pomar 2001a; 2001b; Pomar and Kendall, 2008). Types of carbonate producing biota may also govern the evolution and development of different types of carbonate platform (Pomar et al., 2012a).

Besides these three main factors, other subordinate controls on the temporal and spatial evolution of carbonate platforms include clastic input, temperature, salinity, nutrients, and other physico-chemical variables (Hallock and Schlager, 1986; Weissert et al., 1998; Pomar, 2001a; Mutti and Hallock, 2003; Pomar and Kendall, 2008).

Fault-bounded carbonate platforms are widely occur during Cenozoic in active rift settings (Bosence, 2005) and extensive literature is available for such sites around the world (e.g. Coniglio et al., 1996; Wilson et al., 2000; Pomar et al., 2005 Brandano et al., 2009; Benisek et al., 2010; Hughes, 2014 and references therein). Most of these studies focus on the description of the lithofacies and biofacies, platform geometry, and large-scale depositional sequences. However, less attention has been given to high-resolution sequence architecture (4^{th} or 5^{th} order), the role of evolving rift basin topography and its interaction with the carbonate factory in controlling depositional geometries, and changes between allocyclic and autocyclic controls within the carbonate platform. In this context, autocyclic controls encompass sediment reworking and include variable gravity-driven sedimentary flow types within platform slope deposits.

This study examines the architecture of platform carbonates from three different structural settings within one rift segment of the Early Miocene Red Sea Rift: a) a fault-block hangingwall dipslope, b) the outer platform-top and upper to mid-slope across a normal fault-controlled platform margin, and c) an attached platform developed on a footwall fault-tip within a basin margin structural relay zone. The internal architectures of these carbonates are characterized, with particular attention given to whether or not they exhibit cyclical stratigraphic signatures on scales of a few metres, scales that might represent 4th or 5th order parasequences, separated by marine flooding surfaces (Goldhammer et al., 1993). The relative importance of the major controlling factors are then explored for each of these three structural settings. These examples illustrate the need to consider spatial and temporal variations in local tectonic control of relative base level, as a key factor in understanding syn-rift platform carbonates.

2. GEOLOGICAL FRAMEWORK

The Red Sea developed in response to the Oligo-Miocene separation of the Arabian and African plates (Lyberis, 1988; Bosworth et al., 2005), and Early to Middle Miocene syn-rift formations are exposed across the Midyan Peninsula (Fig. 1), offering the opportunity for detailed lithostratigraphic and structural mapping. Depositional architecture may thus be characterized within a tectonically influenced stratigraphic framework.

The two Early Miocene carbonate units studied here are the Musayr Formation in the west (Sites 1-2, Fig. 1) and the Wadi Waqb Member exposed in the east (site 3 in Fig. 1) and in the south (site 4 in Fig. 1) of the Midyan area, on the NE margin of the present day Red Sea. Although the Wadi Waqb member has previously been identified and details of its micropalaeontology established, only a general sedimentological description has been published for this study area (Dullo et al., 1983; Hughes & Johnson, 2005; Hussain & Al-Ramadan, 2009; Hughes, 2014). The outcrops coincide with structural highs in the area (Kamal and Hughes, 1993; Hughes and Johnson, 2005), a result of rifting during the late Oligocene to Recent (Bosworth and McClay, 2001). A modified lithostratigraphy for this region is presented in Figure 2 and discussed briefly here.

The Proterozoic basement is locally overlain by Lower Cretaceous Adaffa Formation clastics in fault-bounded inliers. Both are post-dated by the first sedimentary unit of the Red Sea Rift in this region, the Al-Wajh Formation. This formed immediately after rifting initiated and consists of immature continental fluvio-lacustrine sediments. The thickness of the coarse-grained siliciclastic Al-Wajh Formation is variable throughout the basin because of the irregularity of fault blocks and underlying basement topography (Tubbs et al., 2014).

Later, the Yanbu and Musayr formations were deposited during the first major marine incursion towards the Midyan Basin. The Musayr Formation therefore represents the first major carbonate unit in the Midyan Basin (Hughes, 2014; Tubbs et al., 2014). The contemporaneous development of the evaporitic Yanbu Formation was due to local basin restriction from open marine circulation.

An apparent increase in subsidence rates compared to sediment supply led to the deposition of the deep marine Burqan Formation, dominated by gravity- and turbidite-flow-driven sediments. Following the Burqan Formation, a period of non-deposition is recognized locally in the study area. As a series of fault blocks subsequently underwent rotation and differential uplift and subsidence due to tectonic reactivation, the second major carbonate succession, the Wadi Waqb Member of the Jabal Kibrit Formation, developed (Hughes & Johnson, 2005; Tubbs et al., 2014). The Jabal Kibrit Formation, deposited across the paleo-highs and adjacent basin during the Early to Middle Miocene (17-17.5 Ma), consists of a mixed carbonate-siliciclastic succession.

3. METHODOLOGY

Fieldwork in the Midyan Peninsula was carried out in early and late 2013, and mid-2014 to examine the most representative and accessible carbonate exposures of the Musayr Formation (represented by two sites in the Maqna and Wadi Al-Hamd areas (Fig. 1) and the Wadi Waqb Member (represented by two sites, at Wadi Waqb itself and at Ad-Dubaybah (Fig. 1). In both studied units, the facies characteristics were described and analyzed through detailed logging of stratigraphic sections and one hundred and eight representative samples were collected for sedimentologic and petrographic analysis. A total of sixty eight samples of the Wadi Waqb Member were collected from the Wadi Waqb and Ad-Dubaybah sites, and forty samples were collected for the Musayr Formation from the Maqna and Wadi Al-Hamd sites. Thin sections were prepared for all samples for microfacies analysis. This study uses the widely known nomenclature of Dunham (1962), later modified by Embry & Klovan (1971), to describe the carbonate rock textures.

4. LITHOFACIES DESCRIPTION

4.1 Musayr Formation (Late Aquitanian)

The studied outcrop locations of the Musayr Formation are restricted to the northwestern part of the Midyan peninsula (sites 1 and Fig. 1). The Maqna half graben lies to the west of the Jabal Tayran fault block high, which displays an east-dipping hangingwall dipslope to the broader half graben controlled by the Red Sea Fault system on the eastern side of the basin (Figs. 1 and 3). Seven lithofacies were recognized in the Musayr Formation.All facies are illustrated in Figures 4 and 5 for the Musayr Formation. Within the Musayr Formation lithofacies (LF1 to LF7) have been distinguished on the basis of components and sedimentary structures and their relative position, from distal (LF1) to proximal settings (LF7).

LF1-Stromatolitic Boundstones

Stromatolitic boundstone is found in the basal part of the sedimentary successions of the Musayr Formation and marked the transition from fluvio-lacustrine Late Oligocene-Early Miocene Al-Wajh Formation to open marine Musayr Formation. The stromatolite is recognized with two different morphologies, planar in the lower part and domal, undulatory shape with slight deformation in the upper part (Fig. 4A). The presence of fractures filled dolomite with dark brown color are also characterized this facies (Fig. 4B).

LF2- Calcareous Sandstones

This facies consists of medium grained, poorly sorted and subangular quartz and feldspar. The presence of medium to thick high angles cross bedding is one of this facies characteristic. Seven paleocurrent measurements on the planar to tabular crossbedding suggest unidirectional distribution towards the east of approximately 80-92°. The preservation of vertical burrows are common in this facies along with the appearance of pebble lenses (Fig. 4C)

LF 3-Foraminiferal-Bioclastic Packstones

This facies is found in the lower part of the sedimentary successions and interbedded with calcareous sandstones facies (LF3). This facies is characterized by dark brown in color with medium to thick parallel bedding. The most abundant component is miliolids foraminifera (Quinqueloculina sp) while other bioclasts such as gastropod and bivalves are the subordinate components (Fig. 4D). This facies is changing laterally to more peloidal rich grainstones towards the basinward.

LF4-Ooidal-Quartz Grainstones

This facies is observed in both measured sedimentary sections suggest good lateral continuity. The ooidal-quartz grainstones facies is characterized by thin to medium well bedded, low angle cross-bedded (Fig. 5A). It is found associated with peloidal grainstones (LF5). The ooids cortex form in concentric arrangements with the nuclei are mostly composed of quartz fragments (Fig. 5B). Allochems are predominantly quartz grains, with subordinate bioclasts and micritic intraclasts.

LF5-Peloidal Grainstones

This facies is mainly composed of peloids and micritized ooids grains (Fig. 5C). It appears thinly bedded in outcrop and interbedded with the ooidal-quartz grainstone facies (LF-4). Variable amounts of silt-sized quartz and minor bioclasts (gastropods, brachiopods) are recognized under the thin section.

LF6-Oyster Rudstones-Floatstones

This facies comprised the most dominant and thick section in the Musayr Formation sedimentary successions. Oyster rudstone and floatstone facies were (Fig. 6D) observed at both study sites. The oyster shells were found broken and fragmented, suggesting that the oysters were reworked and transported from their origin further upslope. Other biocomponents found in this facies are foraminifera and rhodolitic fragments.

LF7-Foraminiferal-Bioclastics Wackestones

This facies mostly comprise ramp-derived fragments. Abundant benthic forams (Miogypsina sp and Miogypsinoides sp), minor bioclasts (bivalves, gastropods) intraclasts and rhodolithic fragments characterize this facies (Fig. 5E). The matrix of this facies is mostly recrystallized into dolomite (Fig. 5F). This facies is associated with the oyster rudstone and found commonly at the base of parasequences (Fig. 8). Bioturbation is also observed in this facies.

4.2 Wadi Waqb Member (Late Burdigalian)

The Wadi Waqb Member is cropping out in two different locations (1) Wadi Waqb, southern part of the Ifal Basin and (2) Ad-Dubaybah, located near the rift margin in eastern part of Midyan Peninsula. From these two locations this study have identified fourteen lithofacies that are distinguished based on their skeletal and non-skeletal components, sedimentary structures and their position in the carbonate platform from proximal (A1) to distal (C4).

A1-Bioclastic-Peloidal Packstones

This facies is observed in the lower part of the sedimentary section, particularly in the Wadi Waqb locality. Low angle-cross bedding is recognized as the prominent sedimentary structures in this facies. The main component of this facies is peloids and bioclasts such as gastropods, echinoids and bivalve (Fig. 6A). This facies exhibit normal grading texture with grain-dominated packstone in the lower part pass into mud-dominated packstone in the upper part. Subordinate basement derived fragments also found incorporated within this lithofacies (Fig. 6B).

A2-Lithoclastic Wackestone-Packstones

This facies is associated with bioclastic-peloidal packstone (A1), observed as thinly bedded succession in the outcrop with outsized reworked limestones boulder incorporated into the facies (Fig. 6C). Similar components with the lithofacies A1 are recognized under the thin section, however, the percentage of lithoclasts such as basement derived fragments and micrite is increasing in this lithofacies.

A3-Planar Cross bedded to Wavy Bedded Foramiferal Packstones-Grainstones

This facies is observed in the middle part of the measured sedimentary section in the Wadi Waqb locality. Planar, low angle cross bedding is recognized in the lower part while wavy bedded is more pronounce in the upper part of this facies. The main component of this facies is benthic forams (rotaliid and ammonia) and bioclasts such as brachiopods, gastropods and bivalve. One of the main characteristic of this facies is the presence of in situ echinoids (Clypeasteroida) (Fig. 6D).

A4-Conglomerates and Conglomeratic Sandstones

Conglomerates and conglomeratic sandstones are recognized in the lower part of the studied section and proximal part of the platform in the Ad-Dubaybah location. This facies is characterized by cobble to pebble sizes, subrounded to well rounded, poor to medium sorted basement derived fragments (Fig. 7A). Five paleocurrent measurements from grain imbrication suggest bidirectional distribution, approximately towards the southwest 225° (n=3) and southeast-south 172° (n=2).

A5-Cross Bedded Calcareous Subarkosic Sandstones

This facies is associated with and deposited above the conglomeratic sandstones (A4). The main components is subangular to subrounded, medium sorted basement derived fragments with quartz and feldspar as the predominant composition. The presence of calcite cements can be observed in thin section. Planar and tabular cross bedding are the main sedimentary structures that exhibit south-southwest direction. Vertical burrows are common within this facies.

A6-Stromatolitic Boundstones

Stromatolitic boundstone is found in the upper part of the sedimentary section from both locations and associated with the calcareous sandstone (A5) in the lower part and ooidal grainstone facies (A7) in the upper part. The stromatolites can be recognized as a patchy, domal and planar shapes (Fig. 7B and 7C). Observation from thin section shows that the microbial laminae is mainly entrapping siliciclastic grains.

A7-Cross Bedded Ooidal Grainstones

This facies occurs in the most upper part of the sedimentary section measured in the proximal part of platform in the Ad-Dubaybah location. Quartz and basement derived fragments act as the nuclei of this ooids (Fig. 7D). Different cortex thicknesses suggest the presence of normal and superficial ooids. Planar cross bedding suggest unidirectional current towards the southwest direction, 210-225° (n=6).

B1-Rhodolithic Packstones-Grainstones

Rhodolitic packstones-grainstones facies is very common in both studied locations. This facies primarily composed of rhodolith (< 2mm), with subordinate bioclasts (brachiopods, bivalves, echinoids, gastropods, and bryozoans), and large benthic foraminifera. The facies exhibit well bedded package with normal grading texture from grainstone to mud dominated packstone. The presence of rhodolith is more abundant in the proximal than distal part (Fig. 7E).

B2-Rhodolithic Wackestones

This facies is found interbedded with rhodolithic packstone to grainstones (B2). The main component is rhodolith with subordinate bioclasts. The presence of localized rhodolith spheres (>5cm) is scattered throughout the facies. Under thin section, the matrix is selectively dolomitized.

B3-Bioclastic-Rhodolithic Floatstones

Bioclastic-Rhodolithic floatstones facies is recognized in the distal part of the Wadi Waqb member succession. This facies primarily composed of bioclasts (brachiopods, bivalves, echinoids, gastropods, and bryozoans) and rhodoliths. Well-bedded package with highly fractured outcrop is the main characteristic of this facies.

B4-Corals Mounds

This facies is observed as in situ in the Ad-Dubaybah locality where the corals are abundant (dominant genera are Porites and Favites) (Fig. 7F), locally bored by bivalves and encrusted by red algae. Based on the field observations, there are three distinct coral morphologies that form coral biostromes (sensu Bosence et al., 1998), patchy-fringing corals and colonies without well-developed framework (sensu Riding, 2002). These types of corals are common in during the Miocene time (Pomar et al., 2012)

C1-Burrowed Bioclastic-Intraclastic Floatstones

This facies is well developed in the Wadi Waqb location and mainly composed of intraclast and bioclast fragments. Vertical burrows are recognized in the outcrop and in thin section where the burrows filled with micrite. The main characteristic of this facies is massive to planar bedded with highly fractured outcrop.

C2-Coral-rich Rudstones

Coral rich rudstones is found associated with bioclastic-intraclastic floatstones facies (C1) but more pronounce in distal part of the platform. The fragmented shape and rotated position of the corals from its original position suggest transportation processes. The outsized corals fragment are ranging from 5 cm to 30 cm in diameter.

C3-Well-cemented Rudstones

This facies is observed and well developed in the Ad-Dubaybah location. The main characteristic of this facies is grain supported and well cemented of rhodolith-corals colonies. This well cemented facies also represent the base of parasequences developed in the Ad-

Dubaybah location (Fig.10). From the outcrop, the rhodolith colonies is increasing towards the distal part while in the proximal part is replaced by coral colonies and becoming smaller in size.

4.3 Facies and Depositional Architecture

Depositional Architecture Musayr Formation

The seven lithofacies are collectively characterized by laterally extensive continuity of facies over hundreds of meters and by the absence of wave-resistant reef frameworks at the studied outcrops. When combined with structural mapping this study implies that deposition of the Musayr Formation occurred on a hangingwall dip-slope carbonate ramp, deepening toward the east (Fig. 8). The Musayr Formation does not exhibit an outer ramp environment towards the basin, instead passing directly from shallow to progressively deeper marine siliciclastics to the east, which can be ascribed lithostratigraphically to the Burqan Formation. Generally, the Musayr Formation represents the first major marine incursion into this segment of the Red Sea rift basin. The carbonate parasequences of the Musayr Formation are revealed by a repetitive pattern of shallowing and an abrupt flooding surface (Fig. 8). Overall, parasequence stacking patterns at the studied outcrops show aggradational to slightly progradational parasequence sets within an inner to middle ramp environment (Fig. 8). The shallowing upward cycles observed in the Musayr Formation are represented by mud-dominated facies in the lower part that represent more distal, low energy middle ramp overlain by progressively higher energy, possibly storm-derived oyster rudstones that represent the more proximal middle ramp (Fig. 8).

Depositional Architecture Wadi Waqb Member (Wadi Waqb)

The Wadi Waqb location is located in the southern part of the Ifal Basin. It represents an uplifted and rotated footwall margin carbonate platform (Fig. 9). This area is surrounded by younger evaporite deposits of the Kial and Mansiyah formations. The lithofacies legend used for the Wadi Waqb member represented in Figure 10.

The stratigraphy and depositional architecture of the Wadi Waqb Member platform are presented in Fig. 11 and a representative field-view is provided in Fig. 9. As described in the results section, these facies represent a series of platform interior and slope deposits. The Wadi Waqb carbonate platform is characterized as an isolated carbonate platform with steep, fault-bounded slopes and similar features are also recognized from the seismic section in the Midyan onshore field (Figs. 11A and B). The major break in slope and the abundance of coral fragments in the slope deposits may suggest the presence of a tropical coral colonies and/or coral biostromes (e.g. scleractinians). This characteristic geometry of tropical carbonate accumulation is directly related to the production and reworking of carbonate debris. The slope deposits likely developed as a result of earthquake-triggered slope collapse in combination with storm wave-generated gravity flows or overloading carbonate production along the margin in conjunction with internal waves impinging on the slope (Pomar et al., 2012b). A random internal architecture is thus apparent, instead of any periodic stacking architecture that might be related to eustatic or tectonic changes. No recognizable parasequences can be traced and identified from this location due to the random facies organization and limitation of the highly fractured outcrop.

Depositional Architecture Wadi Waqb Member (Ad-Dubaybah)

Ad-Dubaybah is located in the eastern part of the Midyan Basin, against the rift shoulder (Fig. 12). It represents a carbonate platform developed on the upthrown side of the tip of one normal fault, in the zone of overlap (soft relay ramp) with respect to the next rift-margin fault to the north. The fault-bounded platform was subsequently separated structurally from the rift footwall, when a hard-linked relay zone joined the two normal fault segments (Fig. 12).

Based on the spatial lithofacies distribution, the Ad-Dubaybah carbonate platform represents an attached, fault-bounded, rimmed shelf located within a relay or transfer zone on the rift margin. The occurrence of siliciclastic-dominated sequences in the platform interior suggests significant siliciclastic input during the depositional period. However, siliciclastics rapidly die out from east to west across the platform, implying that there was an eastwards depositional tilt across the platform. This allowed the siliciclastics to be trapped to the east of the platform and carbonate productivity and coral colonization occured on the western crest of the platform. The repetitive, stacked, shallowing-upward parasequence pattern is recognized in the upper slope to platform margin environments, in an overall combined progradational-aggradational manner (Figs. 13A and B). The parasequences are interpreted as the basic building blocks of the Wadi Waqb carbonate platform at this location. The presence of parasequence cycles varies laterally (east-west) across the platform (Fig. 13), probably due to differences in tectonic displacement rates and differing siliciclastic flux rates from platform crest to the sand fairway to its east. There are two different parasequence cycle building blocks recognized in this area (i) represented by a coarsening upward trend from rhodolithic wackestone, with localized floatstone to rhodolithic grainstone capped by flooding surface in the form of well cemented surface carbonate mostly located in the slope area (Fig. 13A); (ii) mud-dominated wackestone pass into coral mounds and capped by well cemented carbonate. A key feature of this rift margin-attached platform is that the structural configuration allowed clastic sediments to be diverted around the platform high, such that carbonate productivity and preservation was maximized away from the clastic fairways and interfingering occurred into siliciclastics towards the east.

5. DISCUSSION

5.1 Controlling Factors on Carbonate Platform Geometries

Tectonic Activity

The development of the different carbonate platforms described in this study was primarily controlled by the structural evolution of the basin when the carbonates were established (e.g., Fig. 11B). The development of fault block highs segregated clastic fairways from clastics-starved locations where carbonate productivity could be established. In addition, the local tectonic context would have determined local relative base level changes and hence stratal geometries. For example, the fulcrum/pivot location on any tectonically rotating carbonate ramp would have contributed to determining the local stratigraphic geometries, as exemplified by the Musayr Formation case study. If the fulcrum was located above the sea level when downslope subsidence and upslope uplift occurred, it would have increased the accommodation space on the submerged part of the ramp through time and downdip, and tended to develop either (i) retrogradational geometries or (ii) progradational geometries with downward thickening if carbonate production rates were high enough. Alternatively, if the fulcrum was located below sea level, the precursor sediments would have been exposed updip and accommodation space would have decreased above the level of the rotational fulcrum, leading to offlapping stratal geometries. The aggradational to progradational parasequence set geometries of the Musayr Formation (Fig. 8) imply that the local fault block rotational fulcrum lay updip, to the west of the studied outcrops. This exemplifies how tectonic activity played a dominant role in controlling the establishment and the stratal geometries of the carbonate platforms studied, with any orbital forcing-related eustacy being a second order control, only apparent in areas of restricted tectonic displacement rates.

Relative Sea-level

The strong influence of relative sea-level fluctuations has been recorded in many ancient carbonates (e.g., Pomar, 2001a; Pomar et al., 2005; Laya et al., 2013). The Midyan Basin has experienced an overall rise in relative sea level during the Miocene driven by tectonic subsidence, superimposed on high-frequency eustatic fluctuations. The major role of sea level variations in the studied sections would have been in controlling the carbonate factory. During late transgression and highstand conditions, the carbonate factory would have thrived and sediment accumulation may have kept pace with relative sea level rise, tending to develop an aggradational-progradational system. This condition is perhaps best represented by the carbonate platform development of the Wadi Waqb Member, in particular at Ad-Dubaybah (Fig. 13B). Relative sea level falls have led to uppermost platform erosion and inhibition of reef development, but only if rates of eustatic sea level fall exceeded local tectonic subsidence rates (refer to Gawthorpe et al. (1994) and Collier and Gawthorpe (1995) for equivalent discussions related to siliciclastic systems). Enhanced erosion processes during falling stages may have increased the reworking of sediments into the slope area, where they are redeposited as gravity flow sediments (Figs. 11 and 13).

Although the large-scale controls of platform development in the Midyan Basin can be inferred, the mechanisms responsible for transporting carbonate material at the scale of individual gravity flows remain unknown. This study hypothesizes that gravity flow processes may increase either 1) when the upper part of the carbonate platform was subaerially exposed, which may have led to the erosion and transport of carbonate materials towards the slope, or 2) when continued relative sea level rise was associated with an increase in carbonate production that exceeded the platform capacity, causing the platform-top sediment to prograde to the fault-bounded platform edge and become unstable, such that a significant proportion of the material was transported downslope into the basin.

5.2 Variations of Architecture and Cyclicity in Early Miocene Syn-Rift Carbonates

Many authors have described variations in carbonate platform architecture development based on the maritime rift basin of the Gulf of Suez (e.g., Bosence et al., 1998; Cross and Bosence, 2008). This study has found that similar architectures are also recognized in the contiguous Red Sea Rift. The main difference in platform architecture that this study offer is the presence of separate hangingwall dipslope carbonate ramp that pass into shallow-deep marine siliciclastics in the more distal area and the deposition of evaporites inspite of rimmed platform with prominent slope deposits in the footwall area (Fig. 8).

The Musayr Formation outcrops represent a syn-rift hangingwall dipslope carbonate ramp, the deposits of which interfinger with siliciclastics towards the basin (Fig. 8). There are two models proposed by Cross and Bosence (2008) which are based on the origin and development of the platform, distinguished on the basis of syntectonic or post-tectonic context and fulcrum location, which invoke deposition either (i) downdip of the fault-block fulcrum, which will typically create retrogradational depositional geometries, or aggradational to progradational geometries if sediment flux is high relative to accommodation generation, or (ii) updip of the fault-block fulcrum, which will lead to regressive but offlapping depositional geometries driven by relative sea level fall. The Musayr Formation is interpreted to relate to the former structural model. However, the presence of an overall aggradational to progradational stacking pattern of shallowing upward cycles within the Musayr carbonates (Fig. 8) is interpreted as evidence of high (and increasing) carbonate productivity at this time, such that carbonate sediment flux outpaced the temporal increase in accommodation space on the carbonate ramp.

The Wadi Waqb Member located at the Wadi Waqb locality appears to represent a normal fault-controlled isolated carbonate platform (Figs. 11A and Fig. 11B). Thick packages of slope deposits found in this location indicate the availability of accommodation space on the downthrown side of the syn-depositionally active fault. High carbonate productivity on the platform margin and interior could occur because the platform-top was isolated from any significant siliciclastic drainage fairways. The morphology of the footwall-derived slope deposits is progradational, controlled by the morphology and topography of the faulted margin. No cyclicity is evident within the upper to mid-slope deposits (Fig. 11A). The absence of cycles may due to: (i) high carbonate productivity on the platform margin and across the platform-top causing an unstable platform edge and the shedding of excess material onto the slope, obscuring any signal of short-term tectonic or sea level fluctuations;(ii) the location of the carbonate platform possibly being in the middle of a normal fault segment where highest subsidence rates occur, such that again any short-term relative sea-level changes are obscured by the locally and continuously high subsidence rate and/or (iii) the fact that shallowing upward cycles are recorded on the platform top, not on the slope. Toe of slope to basinal settings are also often characterized by cyclicity but to identify cyclicity in carbonate slope deposits is in general very difficult.

The Ad-Dubaybah location represents a different type of carbonate platform of the Wadi Waqb Member (Fig. 13A). The Ad-Dubaybah site is comparable with the Abu Shaar platform, Gulf of Suez (Bosence et al., 1998; Cross and Bosence, 2008). Each represents a relay zone carbonate platform. However, the Ad-Dubaybah location involves the significant local input of siliciclastics compared to the Abu Shaar platform that created an interfingering between carbonate and siliciclastics, presumably related to the nearby position of drainage entry points across the rift shoulder. The occurrence of this carbonate platform is associated with the now hard-linked fault set that creates abrupt topographic changes along the rift margin (Fig. 12) and that allowed the development of an attached carbonate platform with rimmed margin, probably before the rift margin faults became hard-linked. One of the main characteristics of this platform and also the main difference with the Wadi Waqb location is the presence of repetitive shoaling-upward cycles within the outer platform margin to upper slope environments (Fig. 11A). To explain the occurrence of these parasequences at this study site, two mechanisms may be proposed: (i) the superimposition of high frequency sea level fluctuations over some continuous but relatively low rate of tectonic displacement. It is possible to observe the signal of high frequency eustatic sea level variations because the carbonate platform is located towards the tip of the normal fault where low subsidence rates would have occurred. (ii) stick-slip movement on one or both of the normal faults, cycles being driven by such processes as have been described by Smalley et al (1985). Each fault event moves the hangingwall down instantaneously, generating a flooding surface, with the shoaling-up, progradational to aggradational depositional phase representing the period of quiescence before the next seismic event. In the case of the Ad-Dubaybah platform, this would require that seismic displacements on the fault to the east of the platform dominated over any fault displacements on the fault bounding the western side of the platform (Figs. 12 and 13A). To date, this study cannot strictly resolve which forcing mechanism is the more plausible explanation for the presence of cycles in this location. However, the magnitude of accommodation generation implied by each cycle's thickness is too great to be simply related to any one coseismic slip event on a continental normal fault segment.

5.3 Allocyclicity vs. Autocyclicity on Syn-rift Carbonate Platforms

This study explores whether in maritime rift basin carbonate platforms, seismically driven cycles may be responsible for the development of 5th order depositional cycles, resulting from high-frequency syn-sedimentary fault activity that might generate a recurrent motif in carbonate deposition (Satterley, 1996; Benedictis et al., 2007; Hamon and Merzeraud, 2008; Chow et al., 2013).

The estimation of high frequency parasequences order and time span of the Musayr and Wadi Waqb carbonate successions is very difficult because the absent of detailed and precise geochronology and biostratigraphic constrains. Accurate parasequences counting is hindered by the highly faulted outcrops and erosions. This problem has also been encountered from many carbonate platform in the adjacent areas, including Mediterranean platform (e.g., Pomar et al., 2005). Despite this problem, this study try to estimate and speculate the frequency order based on the number of parasequences observed and the time span of each carbonate successions. The Musayr Formation deposited in a maximum time span of 1.7 My and produced at least 8 to 12 high-frequency parasequences (Fig. 8). There are at least 4 to 5 cycles have been recorded in the Wadi Waqb carbonate that deposited within a maximum time span of 0.7 My (Figs. 13A and 13B). Based on this information together with meter-scale cycle thicknesses measured in the outcrops, this study suggest that the parasequences are possibly belong to 5th order depositional cycles (of a magnitude of meters to a few tens of meters) may be accounted for orbitally driven high frequency eustatic fluctuations driven by Milankovitch cycles. This scale of cyclicity may be predicted to occur in the carbonates of the Midyan Basin because the Early Miocene was part of the global icehouse episode, in which eustatic fluctuations were probably a moderately high-amplitude and high-rate phenomenon. Reefs and platforms are particularly sensitive to Milankovitch forcing because they respond to both sea-level cycles and environmental change driven by orbital perturbations (Goldhammer et al., 1990; Schlager, 2005).

This study proposes that interplay between tectonic and eustatically induced allocyclic cycles in these carbonate platforms are only apparent (as typically 5-8m thick parasequences) in the middle ramp of the Musayr Formation and in the upper slope and platform margin deposits of specific locations within the Wadi Waqb Member, locations where syn-depositional tectonic displacements may have occurred at low rates. This allocyclicity is represented by repetitive shallowing upward parasequences separated by flooding surfaces. The relationship between parasequence expression and the lateral variation in tectonic displacement rates in these carbonate platforms is analogous to that described for syn-rift siliciclastic successions by Gawthorpe et al. (1994) and Collier & Gawthorpe (1995). Prominent lateral variations in number and thickness of parasequences are recognized in the Ad-Dubaybah site (Figs. 13A and B) numbers increasing from the platform interior towards the upper slope environment. This phenomenon can be explained by the variation in accommodation space created by the differing magnitude and rates of tectonic subsidence throughout the platform.

6. CONCLUSIONS

This study presents the reconstruction of new depositional models and an assessment of the internal architecture for the Upper Miocene carbonate platforms (of the Musayr Formation (Late Aquitanian) and of the Wadi Waqb Member (Late Burdigalian) of the Red Sea Rift, NW Saudi Arabia. Carbonates were developed on fault block highs, contemporaneous with siliciclastic deposition within the structurally controlled deeper hangingwall fairways. The exposed Upper Miocene carbonate platforms illustrate distinct platform geometries within an extensional tectonic setting. The Musayr Formation example was deposited as a homoclinal carbonate ramp environment, located on the hangingwall dipslope of a syn-depositionally active half graben, where coralline red algae and large benthic foraminifera were the main carbonate producers. The Wadi Waqb Member is here interpreted as having been developed on fault-bounded, carbonate platforms, located on fault block highs within the Midyan Red Sea rift segment. Slope deposits are characterized by steep bedding geometries (up to 40^{o} dips) and clinoform progradation. Although the Musayr and Wadi Waqb carbonates formed in similar tectonic and climatic settings overall, the resulting depositional geometries are distinct from one another, due to contrasting local basin structure contexts and differences in their carbonate factories.

Parasequence-scale cyclicities related to periodic rise and fall of relative sea level may result from eustatic forcing or potentially from cycles of co-seismic displacement in areas close to major active faults. Parasequence sets are observed on a hangingwall dipslope carbonate ramp of the Musayr Formation and in platform edge and upper slope deposits of the Wadi Waqb Member at the Ad-Dubaybah location. Both locations may have been areas of subdued tectonic displacement rate, the latter perhaps due to the net local displacement rate arising from subsidence on a fault to the east and an uplift component from the fault bounding the western side of the platform. This is consistent with there being a greater likelihood of retaining a eustatic expression in stratigraphic architectures in localities where syn-rift tectonic displacement rates and sediment flux rates are minimal. Autochthonous carbonates, including Sclerectinian corals and rhodoliths, may have formed preferentially during periods of relative sea level rise over the platform margin and upper slope due to the space availability that allows the organisms to thrive. High carbonate productivity across the platform-top environments would have allowed progradation and gravitational reworking of material down the slope, across the fault-controlled platform margins. However, allochthonous carbonate resedimentation on the slope may also have been enhanced when the platform-top was subaerially exposed and eroded, whether by tectonic uplift and/or eustatic sea level fall based on the presence of vuggy porosity in the platform-top successions. At the first order, the architectures of these fault-bounded carbonate platforms are primarily due to syn-rift fault activity, with a superimposed low magnitude eustatic signal only locally evident. The tectonic activity was induced by fault block motion and rotation during extension. This activity governed the position of the platforms, their geometries, and the creation of accommodation space across the basin, and hence provided a fundamental control upon the location and nature of carbonate factories.

ACKNOWLEDGMENTS

The authors would like to acknowledge the support provided by King Abdulaziz City for Science and Technology (KACST) through the National Science and Technology Initiative Program (NSTIP) at King Fahd University of Petroleum and Minerals (KFUPM) for funding this project (NSTIP # 11-OIL2145-04). We also thank the Earth Sciences Department at KFUPM for providing the necessary laboratory equipment and analyses for this study. We greatly appreciated the helped of Dr. Dave Cantrell in giving an initial review and fruitful discussions. Sincere thanks to Profs. Luis Pomar, Dan Bosence, George Dix for providing constructive reviews and discussions on earlier version of the manuscript. Editor Octavian Catuneanu, Piero Gianolla and two anonymous reviewers are acknowledge for their constructive comments.

REFERENCES

Benedictis, D. D., Bosence, D., & Waltham, D. (2007). Tectonic control on peritidal carbonate parasequence formation: an investigation using forward tectono-stratigraphic modelling. Sedimentology, **54(3)**, 587-605.

Benisek, M.-F., Marcano, G., Betzler, C. & Mutti, M. (2010). Facies and Stratigraphic Architecture of a Miocene Warm-Temperate to Tropical Fault-Block Carbonate Platform, Sardinia (Central Mediterranean Sea), in Carbonate Systems during the Oligocene-Miocene Climatic Transition (eds M. Mutti, W. Piller and C. Betzler), Wiley-Blackwell, Oxford, UK, 129-148.

Bosence, D., Cross, N., & Hardy, S. (1998). Architecture and depositional sequences of Tertiary fault-block carbonate platforms; an analysis from outcrop (Miocene, Gulf of Suez) and computer modelling. Marine and Petroleum Geology, 15(3), 203-221.

Bosence, D. (2005). A genetic classification of carbonate platforms based on their basinal and tectonic settings in the Cenozoic. Sed. Geol., **175(1)**, 49-72.

Bosworth, W. & K. McClay (2001). Structural and stratigraphic evolution of the Gulf of Suez Rift, Egypt: A synthesis. In P.A. Ziegler, W. Cavazza, A.H.F. Robertson and S. Crasquin-Soeau (Eds.), Peri-Tethyan Rift/Wrench Basins and Passive Margins. Memoir Musee Naturale Histoire, Peri-Tethys Memoir, **186 (6)**, 567-606.

Bosworth, W., Huchon, P., & McClay, K. (2005). The Red Sea and Gulf of Aden basins. J. Afr. Earth Sci., **43(1)**, 334-378.

Bover-Arnal, T., Salas, R., Moreno-Bedmar, J. A., & Bitzer, K. (2009). Sequence stratigraphy and architecture of a late Early–Middle Aptian carbonate platform succession from the western Maestrat Basin (Iberian Chain, Spain). Sed. Geol., **219(1)**, 280-301.

Brandano, M., Frezza, V., Tomassetti, L., Pedley, M., & Matteucci, R. (2009). Facies analysis and palaeoenvironmental interpretation of the late Oligocene Attard Member (lower Coralline Limestone Formation), Malta. Sedimentology, **56(4)**, 1138-1158.

Carr, I. D., Gawthorpe, R. L., Jackson, C. A., Sharp, I. R., & Sadek, A. (2003). Sedimentology and sequence stratigraphy of early syn-rift tidal sediments: the Nukhul Formation, Suez Rift, Egypt. J. Sed. Res., **73(3)**, 407-420.

Chen, D., Tucker, M. E., Jiang, M., & Zhu, J. (2001). Long-distance correlation between tectonic-controlled, isolated carbonate platforms by cyclostratigraphy and sequence stratigraphy in the Devonian of South China. Sedimentology, **48(1)**, 57-78.

Chow, N., George, A. D., Trinajstic, K. M., & Chen, Z. Q. (2013). Stratal architecture and platform evolution of an early Frasnian syn-tectonic carbonate platform, Canning Basin, Australia. Sedimentology, **60(7)**, 1583-1620.

Clark, M.D. (1986). Explanatory Notes to the Geologic Map of the Al Bad' Quadrangle, sheet 28A, Kingdom of Saudi Arabia. Saudi Arabian Deputy Ministry for Mineral Resources Geoscience Map Series GM-81A, C, scale 1:250,000, with text, 46 p.

Collier, R.E.Ll. & Gawthorpe, R.L. (1995). Neotectonics, drainage and sedimentation in central Greece: Insights into coastal reservoir geometries in syn-rift sequences. In: Lambiaise, J.J. (Ed.), Hydrocarbon Habitat in Rift Basins, Geol. Soc. London Spec. Publ., no. **80**, 165-181.

Coniglio, M., N.P. James & D.M. Assaoui (1996). Abu Shaar complex (Miocene) Gulf of Suez, Egypt: Deposition and diagenesis in an active rift setting. In E.K. Franseen, M. Esteban, W.C. Ward and J.-M. Rouchy (Eds.), Models for carbonate stratigraphy from Miocene reef complexes of Mediterranean regions. SEPM Spec. Publ., **5**, 367-384.

Cross, N. E., Purser, B. H., & Bosence, D. W. J. (1998). The tectono-sedimentary evolution of a rift margin carbonate platform: Abu Shaar, Gulf of Suez, Egypt. In Sedimentation and Tectonics in Rift Basins Red Sea:-Gulf of Aden (pp. 271-295). Springer Netherlands.

Cross, N. E., & Bosence, D. W. J. (2008). Tectono-sedimentary models for rift-basin carbonate systems. Controls on Carbonate Platform and Reef Development Edited by Jeff Lukasik and J.A. (Toni) Simo. SEPM Spec. Publ., **89**, 83-105.

Dorobek, S. L. (2008). Tectonic and depositional controls on syn-rift carbonate platform sedimentation. Controls on Carbonate Platform and Reef Development Edited by Jeff Lukasik and J.A. (Toni) Simo., SEPM Spec. Publ., **89**, 57-81.

Dullo, W. C., Hötzl, H., & Jado, A. R. (1983). New stratigraphical results from the Tertiary sequence of the Midyan area, NW Saudi Arabia. Contributions to the geology of the eastern margin of the Red Sea No. 1 A joint DFG-UPM-Project; Publication No. 5 of SFB 108. Newsletters on Stratigraphy, 75-83.

Dunham RJ. (1962). Classification of carbonate rocks according to their depositional texture. In: Ham WE, editor. Classification of Carbonate Rocks, AAPG Mem., **1**, 108– 21.

Embry AF, Klovan JE. (1971). A Late Devonian reef tract on northeastern Banks Island. Bull. Can. Petrol. Geol., **19**,730– 81.

Flügel, E. (2004). Microfacies of Carbonate Rocks: Analysis, Interpretation and Application, Springer-Verlag, Berlin, 984 p.

Gawthorpe, R. L., Fraser, A. J., & Collier, R. E. L. (1994). Sequence stratigraphy in active extensional basins: implications for the interpretation of ancient basin-fills. Mar. Petrol. Geol., **11(6)**, 642-658.

Gawthorpe, R. L., & Leeder, M. R. (2000). Tectono-sedimentary evolution of active extensional basins. Basin Res., **12(3-4)**, 195-218.

Ginsburg, R.N., (1971). Landward movement of carbonate mud: new model for regressive cycles in carbonates. AAPG Bull., **55**, 340.

Goldhammer, R. K., Dunn, P. A., & Hardie, L. A. (1990). Depositional cycles, composite sea-level changes, cycle stacking patterns, and the hierarchy of stratigraphic forcing: examples from Alpine Triassic platform carbonates. Geol. Soc. Am. Bull., **102(5)**, 535-562.

Goldhammer, R. K., Lehmann, P. J., & Dunn, P. A. (1993). The origin of high-frequency platform carbonate cycles and third-order sequences (Lower Ordovician El Paso Gp, west

Texas): constraints from outcrop data and stratigraphic modeling. Journal of Sedimentary Research, 63(3).

Gómez-Pérez, I., Fernández-Mendiola, P. A., & García-Mondéjar, J. (1999). Depositional architecture of a rimmed carbonate platform (Albian, Gorbea, western Pyrenees). Sedimentology, **46(2)**, 337-356.

Hallock, P., & Schlager, W. (1986). Nutrient excess and the demise of coral reefs and carbonate platforms. Palaios, 389-398.

Hamon, Y., & Merzeraud, G. (2008). Facies architecture and cyclicity in a mosaic carbonate platform: effects of fault-block tectonics (Lower Lias, Causses platform, south-east France). Sedimentology, **55(1)**, 155-178.

Hughes, G.W. & R.S. Johnson (2005). Lithostratigraphy of the Red Sea Region. GeoArabia, **10 (3)**, 49-126.

Hughes, G.W., (2014). Micropalaeontology and palaeoenvironments of the Miocene Wadi Waqb carbonate of the northern Saudi Arabian Red Sea. GeoArabia, **19(4)**, 59-108

Hussein, M. & K. Al-Ramadan. (2009). Microfacies analysis of Wadi Waqb Member (Miocene) in Wadi Aynunah, northwest of Saudi Arabia. Carbonates and Evaporites, **24**, 139-149.

Jackson, M. P. A., Hudec, M. R., & Hegarty, K. A. (2005). The great West African Tertiary coastal uplift: Fact or fiction? A perspective from the Angolan divergent margin. Tectonics, **24(6)**.

James, N. P. (1983). Shelf-slope break in fossil carbonate platforms: an overview. The Shelfbreak. Edited by Daniel Jean Stanley and George T. Moore. SEPM Special Publications 33,189-206

Kamal, R.A. & G.W. Hughes 1993. The Ad Dubaybah reef complex, Midyan area, NW Saudi Arabia. Geological Research and Development Division, Miscellaneous Report #1009.

Kendall, C. G. S. C., & Schlager, W. (1981). Carbonates and relative changes in sea level. Mar. Geol., **44(1)**, 181-212.

Kerans, C., & Tinker, S. W. (1997). Sequence stratigraphy and characterization of carbonate reservoirs (p. 130). SEPM Short Course No. 40

Laya, J. C., Tucker, M. E., & Perez-Huerta, A. (2013). Metre-scale cyclicity in Permian ramp carbonates of equatorial Pangea (Venezuelan Andes): Implications for sedimentation under tropical Pangea conditions. Sed. Geol., **292**, 15-35.

Leeder, M. R., & Gawthorpe, R. L. (1987). Sedimentary models for extensional tilt-block/half-graben basins. Continental Extensional Tectonics. Edited by M.P Coward, J.F Dewey and P.L Hancock. Geol. Soc. London Spec. Publ., **28(1)**, 139-152.

Lyberis, N. (1988). Tectonic evolution of the Gulf of Suez and the Gulf of Aqaba. Tectonophysics, **153(1)**, 209-220.

Mack, G. H., Leeder, M. R., & Perez-Arlucea, M. (2009). Late Neogene rift-basin evolution and its relation to normal fault history and climate change along the southwestern margin of the Gerania Range, central Greece. Geol. Soc. Am. Bull., **121(5-6)**, 907-918.

Merino-Tomé, Ó, Della Porta, G., Kenter, J. A., Verwer, K., Harris, P. M., Adams, E. W., & Corrochano, D. (2012). Sequence development in an isolated carbonate platform (Lower Jurassic, Djebel Bou Dahar, High Atlas, Morocco): influence of tectonics, eustacy and carbonate production. Sedimentology, **59(1)**, 118-155.

Moore, C. H. (2001). Carbonate Reservoirs: Porosity, Evolution & Diagenesis In A Sequence Stratigraphic Framework: Porosity Evolution and Diagenesis in a Sequence Stratigraphic Framework, **55**. Elsevier.

Mutti, M., & Hallock, P. (2003). Carbonate systems along nutrient and temperature gradients: some sedimentological and geochemical constraints. Int. J. Earth Sci., **92(4)**, 465-475.

Pomar, L. (2001a). Types of carbonate platforms, a genetic approach. Basin Res., **13**, 313-334.

Pomar, L. (2001b) Ecological control of sedimentary accomodation: evolution from a carbonate ramp to rimmed shelf, Upper Miocene, Balearic Islands. Palaeogeogr. Palaeoclimatol. Palaeoecol., **175**, 249-272.

Pomar, L., Gili, E., Obrador, A., & Ward, W. C. (2005). Facies architecture and high-resolution sequence stratigraphy of an Upper Cretaceous platform margin succession, southern central Pyrenees, Spain. Sed. Geol., **175(1)**, 339-365.

Pomar, L. & Kendall, C. G. S. C. (2008). Architecture of carbonate platforms: a response to hydrodynamics and evolving ecology. Controls on Carbonate Platform and Reef Development. Edited by Jeff Lukasik and J.A. (Toni) Simo. SEPM Spec. Publ., **89**, 187-216.

Pomar, L., Bassant, P., Brandano, M., Ruchonnet, C., & Janson, X. (2012a). Impact of carbonate producing biota on platform architecture: Insights from Miocene examples of the Mediterranean region. Earth-Sci. Rev., **113(3)**, 186-211.

Pomar, L., Morsilli, M., Hallock, P., & Bádenas, B. (2012b). Internal waves, an under-explored source of turbulence events in the sedimentary record. Earth-Science Reviews, 111(1), 56-81.

Pomar, L., Mateu-Vicens, G., Morsilli, M., & Brandano, M. (2014). Carbonate ramp evolution during the Late Oligocene (Chattian), Salento Peninsula, southern Italy. Palaeogeogr. Palaeoclimatol. Palaeoecol., **404**, 109-132.

Read, J. F. (1982). Carbonate platforms of passive (extensional) continental margins: types, characteristics and evolution. Tectonophysics, **81(3)**, 195-212.

Read, J.F. (1985) Carbonate Platform Models. AAPG Bull., **69**, 1-21.

Riding, R. (2002). Structure and composition of organic reefs and carbonate mud mounds: concepts and categories. Earth-Science Reviews, 58(1), 163-231.

Sarg, J. F. (1988). Carbonate sequence stratigraphy. In C.K Wilgus, B.S Hastings, C.G.St.C Kendall, H.W Posamentier, C.A Ross, J.C Van Wagoner (Eds.), SEPM Spec. Publ., 42, pp. 155–181

Satterley, A. K. (1996). Cyclic carbonate sedimentation in the Upper Triassic Dachstein Limestone, Austria: the role of patterns of sediment supply and tectonics in a platform-reef-basin system. J. Sed. Res., **66(2)**.

Satterley, A. K. (1996). The interpretation of cyclic successions of the Middle and Upper Triassic of the Northern and Southern Alps. Earth-Sci. Rev., **40(3)**, 181-207.

Schlager, W. (1992). Sedimentology and sequence stratigraphy of reefs and carbonate platforms. Continuing Education Course Note Series #34, AAPG, 71 pp.

Schlager, W. (2005) Carbonate Sedimentology and Sequence Stratigraphy, SEPM Concepts in Sedimentology and Paleontology: **8**, 200 pp.

Smalley, R. F., Turcotte, D. L., & Solla, S. A. (1985). A renormalization group approach to the stick-slip behavior of faults. J. Geophys. Res.: Solid Earth (1978–2012), **90(B2)**, 1894-1900.

Strasser, A., Pittet, B., Hillgärtner, H., & Pasquier, J. B. (1999). Depositional sequences in shallow carbonate-dominated sedimentary systems: concepts for a high-resolution analysis. Sed. Geol., **128(3)**, 201-221.

Steel, R. J. (1993). Triassic–Jurassic megasequence stratigraphy in the Northern North Sea: rift to post-rift evolution. In Geological Society, London, Petroleum Geology Conference series **4**, 299-315.

Tubbs, R.E., H.G. Aly Fouda, A.M. Afifi, N.S. Raterman, G.W. Hughes & Y.K. Fadolalkarem. (2014). Midyan Peninsula, northern Red Sea, Saudi Arabia: Seismic imaging and regional interpretation. GeoArabia, **19(3)**, 165-184.

Tucker, M. E. (1985). Shallow-marine carbonate facies and facies models. Sedimentology Recent Developments and Applied Aspects. Edited by P. J. Brenchley & B. P. J. Williams Geol. Soc. London Spec. Publ., **18(1)**, 147-169.

Weissert, H., Lini, A., Föllmi, K. B., & Kuhn, O. (1998). Correlation of Early Cretaceous carbon isotope stratigraphy and platform drowning events: a possible link? Palaeogeogr. Palaeoclimatol. Palaeoecol., **137(3)**, 189-203.

Wilson, J.L. (1975). Carbonate Facies in Geologic History. Springer, Berlin, 471 pp.

Wilson, M. E., Bosence, D. W., & Limbong, A. (2000). Tertiary syntectonic carbonate platform development in Indonesia. Sedimentology, **47(2)**, 395-419.

Wilson, M. E. (2002). Cenozoic carbonates in Southeast Asia: implications for equatorial carbonate development. Sed. Geol., **147(3)**, 295-428.

Figure and Table Captions

Figure 1. Landsat image of the Red Sea and Gulf of Aden area (after Bosworth et al., 2005). Geological map of the study area, the Midyan Basin, NW Saudi Arabia (modified after Tubbs et al., 2014). This study focuses on four locations represented in the figure. Sites 1-2: The Maqna and Wadi Al-Hamd areas, which expose the Musayr Formation. Sites 3-4: Ad-Dubaybah and Wadi Waqb outcrops, respectively, of the Wadi Waqb Member.

Figure 2. Generalized lithostratigraphy of the Midyan area. It shows that the Musayr Formation unconformably overlies the Al-Wajh Formation and is laterally equivalent to Yanbu and Burqan formations. Wadi Waqb member of Jabal Kibrit Formation is unconformably overlain the Burqan Formation (modified after Hughes and Johnson, 2005, and Tubbs et al., 2014).

Figure 3. Well-exposed Musayr Formation in the Maqna area (site 1, Fig. 1) directly overlying the siliciclastic Al-Wajh Formation. Post-depositional faults with NW-SE orientation were observed in the outcrop.

Figure 4. Macro- and microscopic features of Musayr Formation facies. **A.** Dark brown stromatolite boundstone facies, occurring as two different morphologies, with planar and domal shapes. **B.** Light grey stromatolite facies intruded by dark brown fracture-filling dolomite. **C.** Calcareous sandstone facies with pebble-cobble lenses, which alternate with wackestone-packstone facies. **D.** Foraminiferal packstone facies characterized by the presence of miliolid foraminifera.

Figure 5. Macro- and microscopic features of Musayr Formation facies. **A**. Well-bedded grainstone succession, comprising oolitic grainstones and a thin bed of peloidal grainstone **B**. Oolitic grainstone. The nuclei consist of quartz grains. Sutured contacts are commonly observed in this facies and suggest deep burial and/or chemical compaction. **C**. Peloidal grainstone-packstone, found associated with the ooidal grainstone. **D**. Oyster rudstone, likely

formed as a product of storm processes. **E**. Rhodoliths, commonly found as fragments and as an encrusting agent. **F**. Recrystallized matrix within oyster-rich rudstone.

Figure 6. Macro- and microscopic features of Wadi Waqb Member facies.

A. Bioclastic packstone with abundant intragranular and moldic porosities characterizing the matrix of bioclastic rudstones recognized in the middle slope environment. **B.** Inclusion of basement fragments in the rhodolitic grainstone facies in the upper slope environment. **C.** Reworked boulder of limestone with vuggy porosity found in the platform interior. **D**. Echinoids (sand dollars) found in their living position and typically recognized within the platform interior.

Figure 7. A. Conglomeratic sandstone facies, found in the basal part of Wadi Waqb Member succession at Ad-Dubaybah. **B.** Microbial laminites with planar bedding found in the uppermost part of the platform interior section. **C**. Stromatolite boundstone facies showing clear laminations. **D**. Ooidal grainstone with concentric cortices and nuclei primarily composed of basement-derived fragments. **E**. Rhodolith colonies found in the proximal part of the platform and showing a decrease trend towards the distal part. This facies is common at the Ad-Dubaybah site. **F**. In situ corals colonies deposited and preserved in their original living position, surrounded by detrital limestone and siliciclastic.

Figure 8. Stratigraphic sections measured from three different localities (see map). Shallowing upward cycles were recognized in the middle to upper part. Depositional architecture of the Musayr Formation a hangingwall dipslope carbonate ramp, deposits of which interfinger with siliciclastics towards the basin.

Figure 9. Field-view of approximately 700 m long, isolated late syn-rift carbonate platform of the Wadi Waqb Member at the Wadi Waqb locality. This shows the Wadi Waqb Member was

deposited unconformably on top of Neoproterozoic basement. Fault 082/55 S, with a brecciated fault zone is visible, as are pervasively dolomitized carbonates on the hanging wall side.

Figure 10. Lithology and sedimentary structure legends for the Wadi Waqb Member sedimentary sections (Wadi Waqb and Ad-Dubaybah sites).

Figure 11. A. Stratigraphic sections measured at the Wadi Waqb locality of Wadi Waqb Member. The sections show high lateral variability from platform interior to middle slope environments. Based on facies variation and architecture, this area represent an isolated, fault-bounded carbonate platform. **B.** Line drawing of seismic section on the Midyan onshore field showing isolated carbonate platform of the Wadi Waqb Member (after Tubbs et al., 2014). Thick slope deposits are also recognized from the seismic.

Figure 12. Field photograph and satellite image showing the geometry of the Ad-Dubaybah locality where the carbonate platform is located adjacent to Proterozoic basement complex.

Figure 13. A. Four stratigraphic sections from the Ad-Dubaybah locality, which represent different depositional environments from beach to platform slope. This area is located in the currently hard-linked relay zone between two rift margin normal fault segments. **B**. Field photo and sketch of the prograding clinoform features. It indicates also a variation in thickness and number of cycles from the platform margin towards the slope.

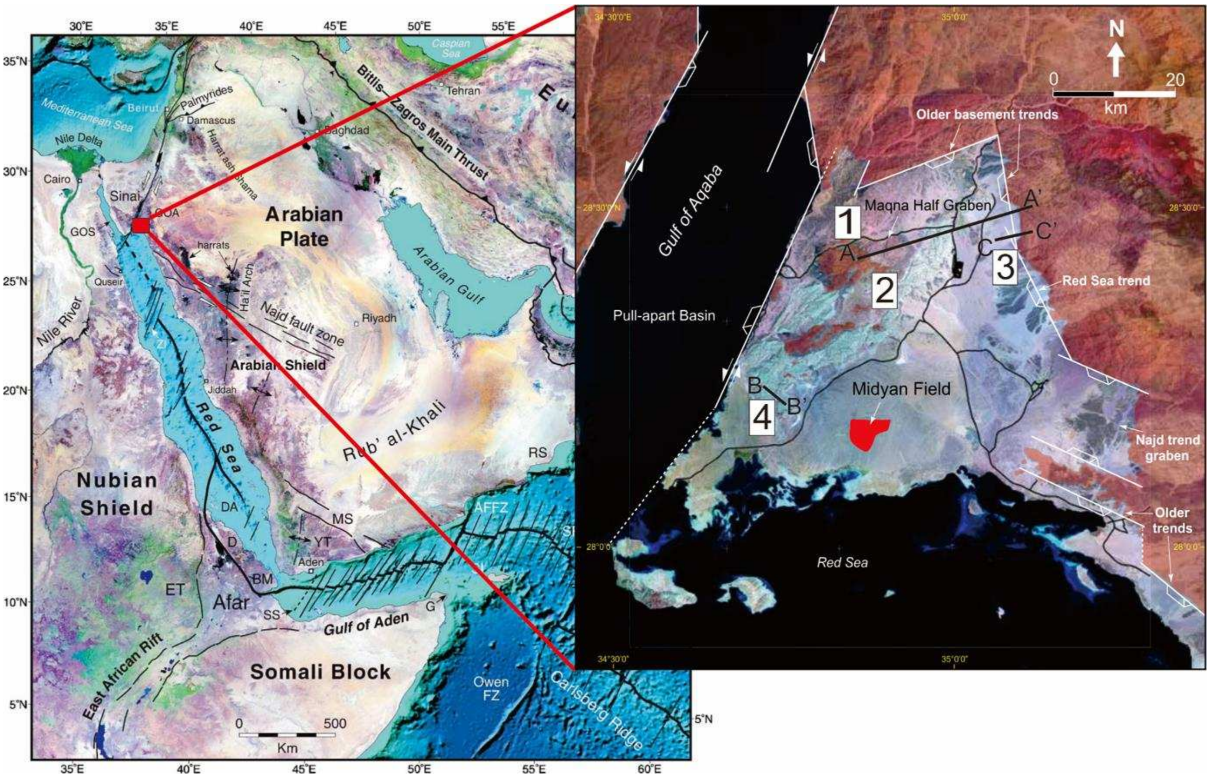

Arabian Plate
Nubian Shield
Somali Block
Afar
Red Sea
Gulf of Aden
East African Rift
Arabian Shield
Rub' al-Khali
Arabian Gulf
Najd fault zone
Bitlis-Zagros Main Thrust
Sinai
GOS
GOA
Cairo
Nile Delta
Nile River
Mediterranean Sea
Beirut
Damascus
Palmyrides
Baghdad
Tehran
Caspian Sea
Riyadh
Jiddah
Aden
Quseir
harrats
Ha'il Arch
Harrat ash Shama
DA
D
BM
ET
SS
MS
YT
RS
G
AFFZ
Owen FZ
Carlsberg Ridge
Km
0
500
Gulf of Aqaba
Pull-apart Basin
Maqna Half Graben
Older basement trends
Red Sea trend
Najd trend graben
Older trends
Midyan Field
N
km
0
20
1
2
3
4
A
A'
B
B'
C
C'

Figure. 1

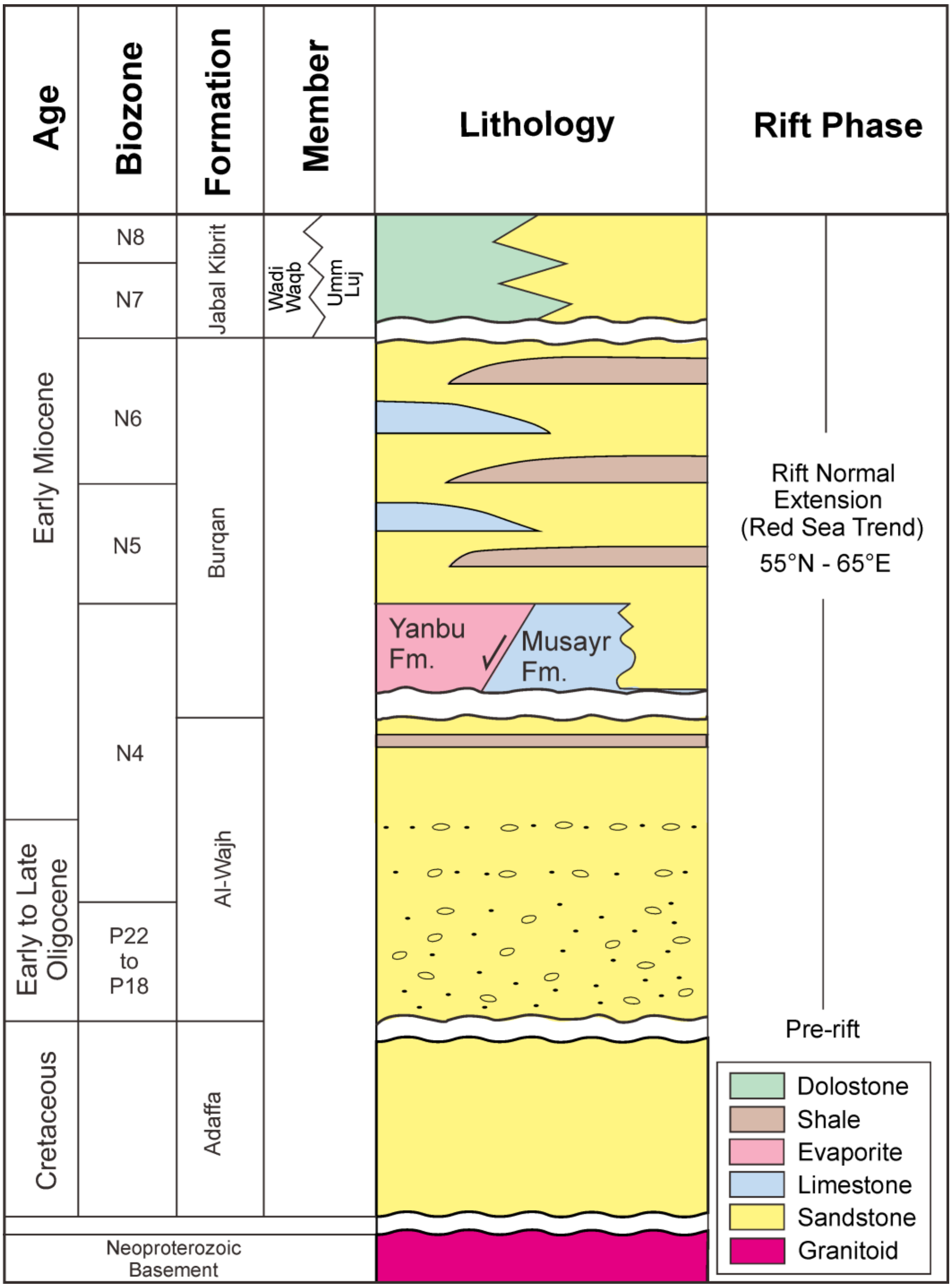

Age
Biozone
Formation
Member
Lithology
Rift Phase
Early Miocene
Early to Late Oligocene
Cretaceous
N8
N7
N6
N5
N4
P22 to P18
Jabal Kibrit
Burqan
Al-Wajh
Adaffa
Wadi Waqb
Umm Luj
Yanbu Fm.
Musayr Fm.
Neoproterozoic Basement
Rift Normal Extension (Red Sea Trend)
55°N - 65°E
Pre-rift
Dolostone
Shale
Evaporite
Limestone
Sandstone
Granitoid

Figure. 2

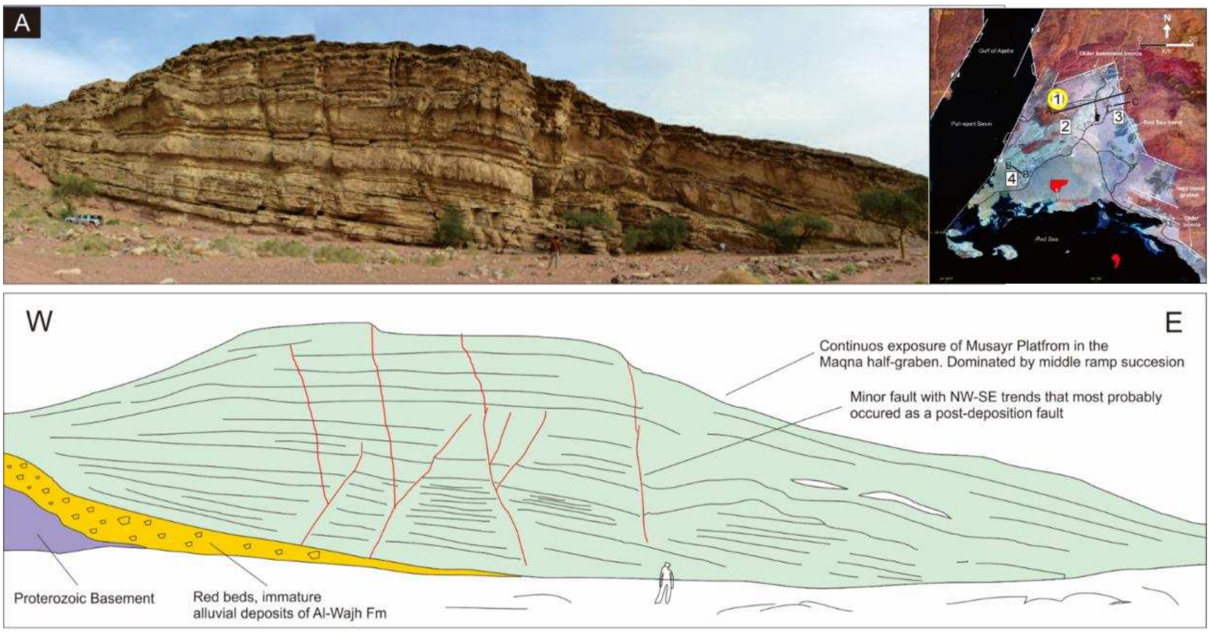
A
W
E
Continuos exposure of Musayr Platfrom in the Maqna half-graben. Dominated by middle ramp succesion
Minor fault with NW-SE trends that most probably occured as a post-deposition fault
Proterozoic Basement
Red beds, immature alluvial deposits of Al-Wajh Fm

Figure. 3

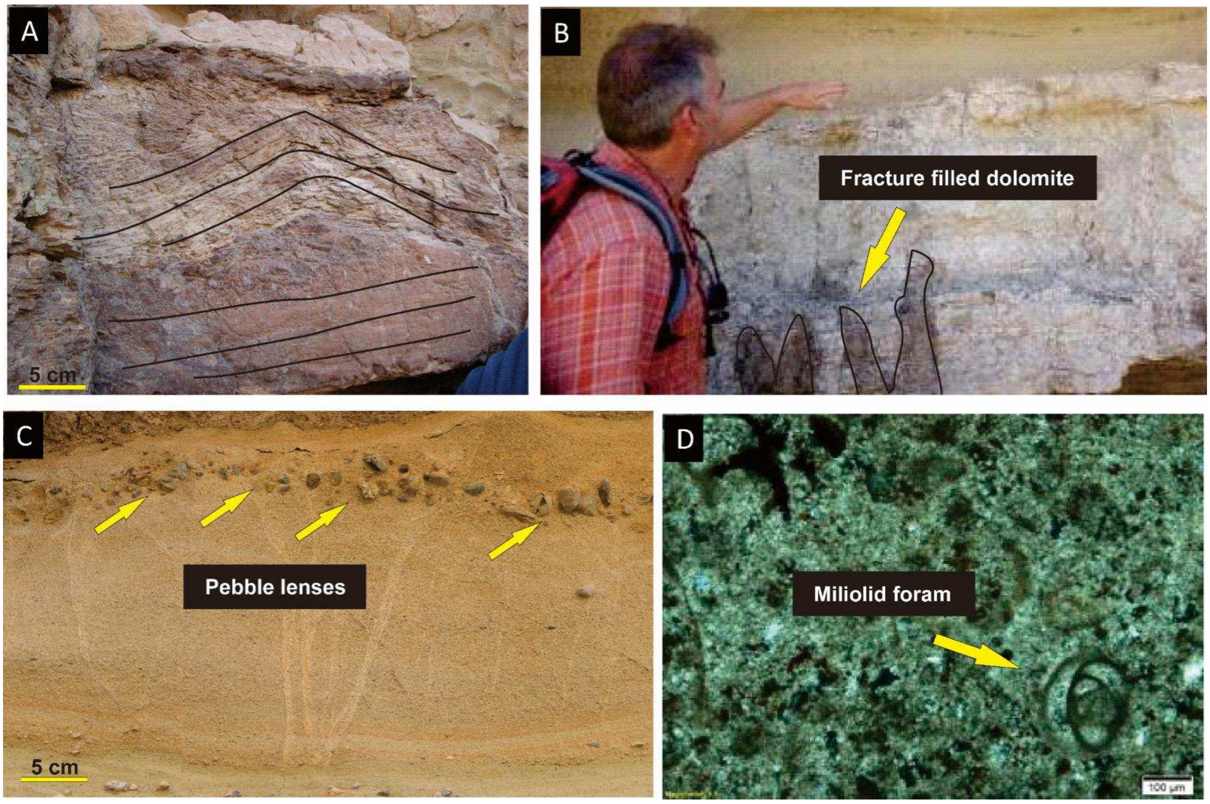
A
5 cm
B
Fracture filled dolomite
C
Pebble lenses
5 cm
D
Miliolid foram
100 µm

Figure. 4

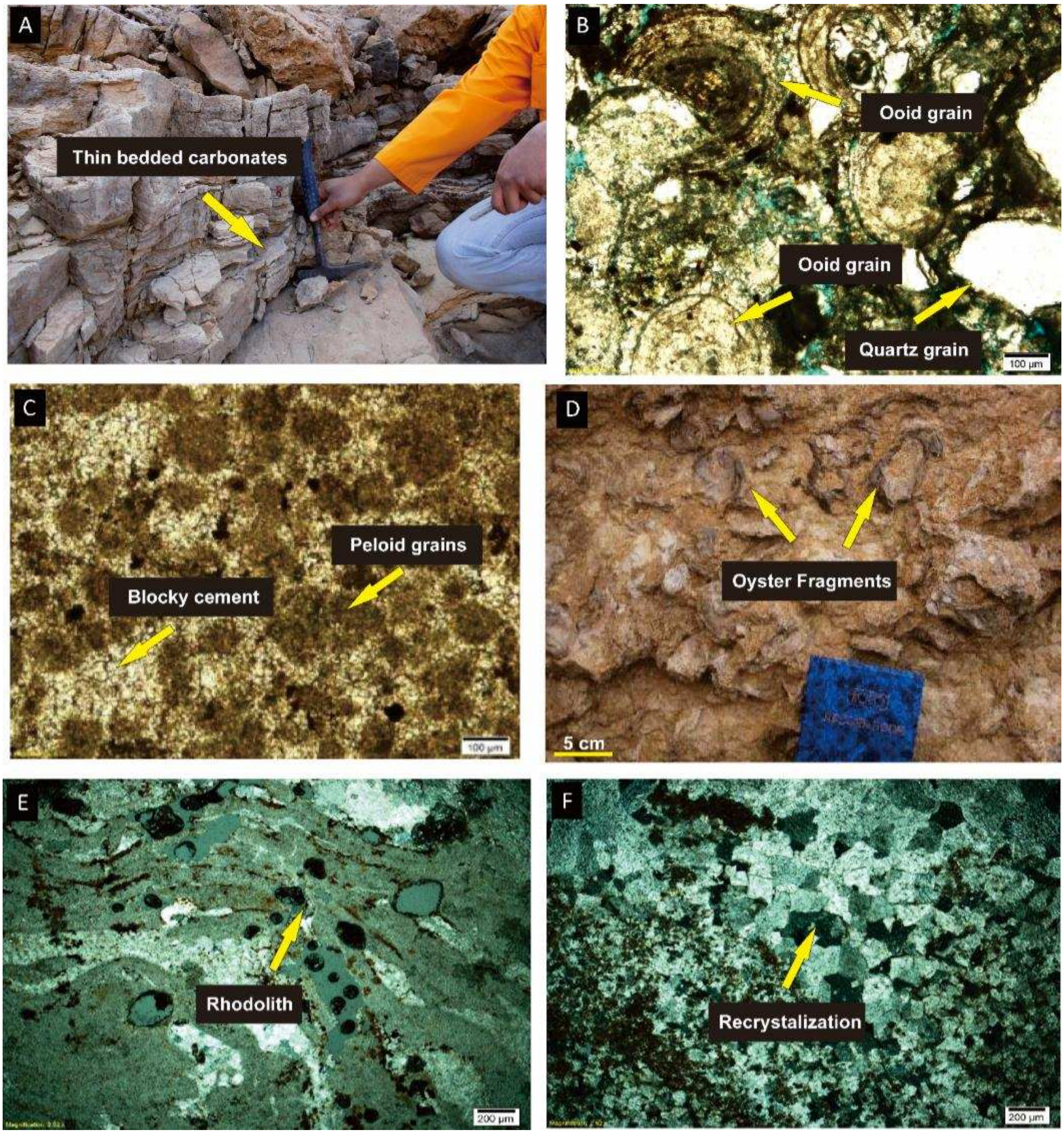
A
Thin bedded carbonates
B
Ooid grain
Ooid grain
Quartz grain
100 µm
C
Peloid grains
Blocky cement
100 µm
D
Oyster Fragments
5 cm
E
Rhodolith
200 µm
F
Recrystalization
200 µm

Figure. 5

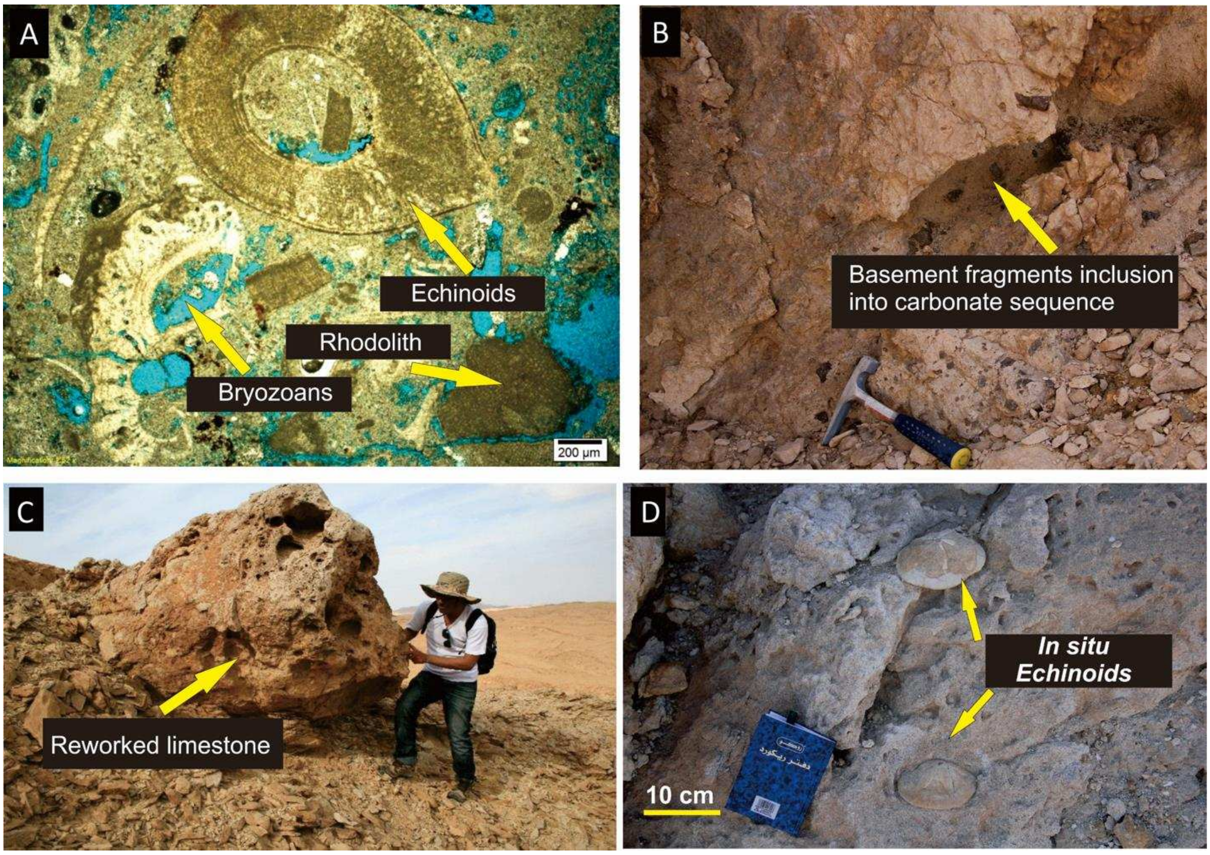
A
Echinoids
Rhodolith
Bryozoans
200 µm
B
Basement fragments inclusion into carbonate sequence
C
Reworked limestone
D
In situ Echinoids
10 cm

Figure. 6

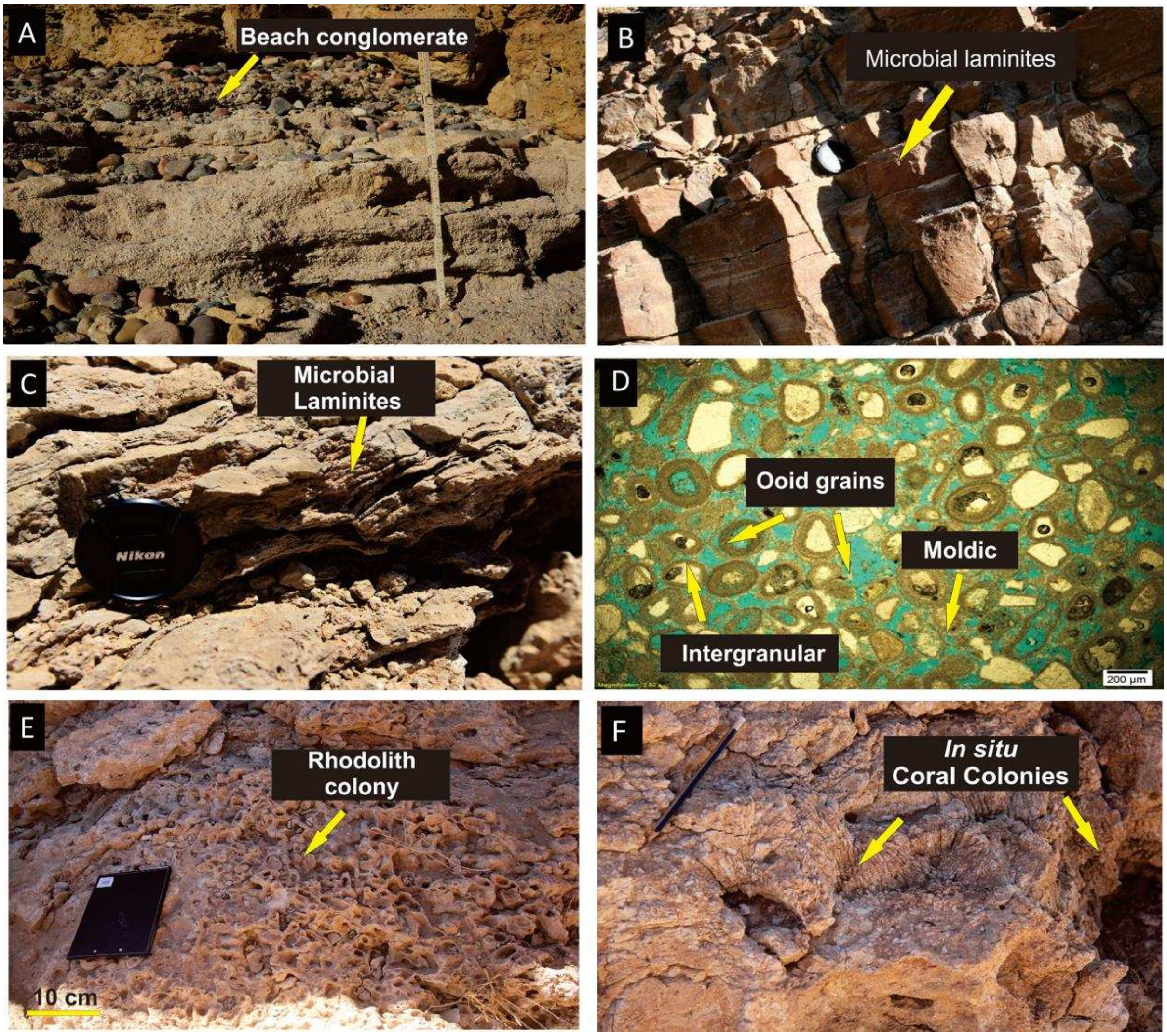
A
Beach conglomerate
B
Microbial laminites
C
Microbial
Laminites
D
Ooid grains
Moldic
Intergranular
200 µm
E
Rhodolith
colony
10 cm
F
In situ
Coral Colonies

Figure. 7

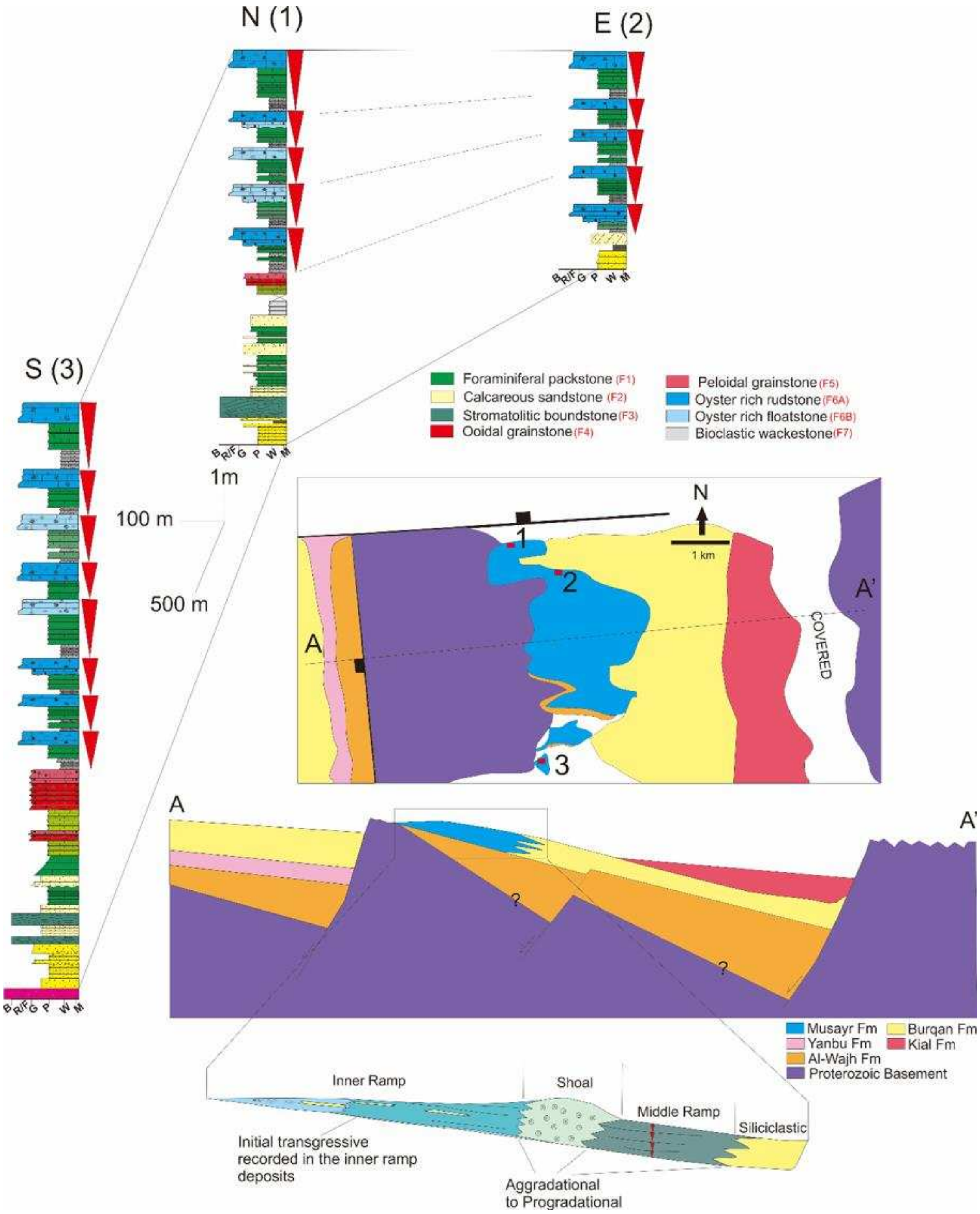

N (1)
E (2)
S (3)
B R/F G P W M
1m
100 m
500 m
Foraminiferal packstone (F1)
Calcareous sandstone (F2)
Stromatolitic boundstone (F3)
Ooidal grainstone (F4)
Peloidal grainstone (F5)
Oyster rich rudstone (F6A)
Oyster rich floatstone (F6B)
Bioclastic wackestone (F7)
N
1 km
1
2
3
A
A'
COVERED
Musayr Fm
Burqan Fm
Yanbu Fm
Kial Fm
Al-Wajh Fm
Proterozoic Basement
Inner Ramp
Shoal
Middle Ramp
Siliciclastic
Initial transgressive
recorded in the inner ramp
deposits
Aggradational
to Progradational

Figure. 8

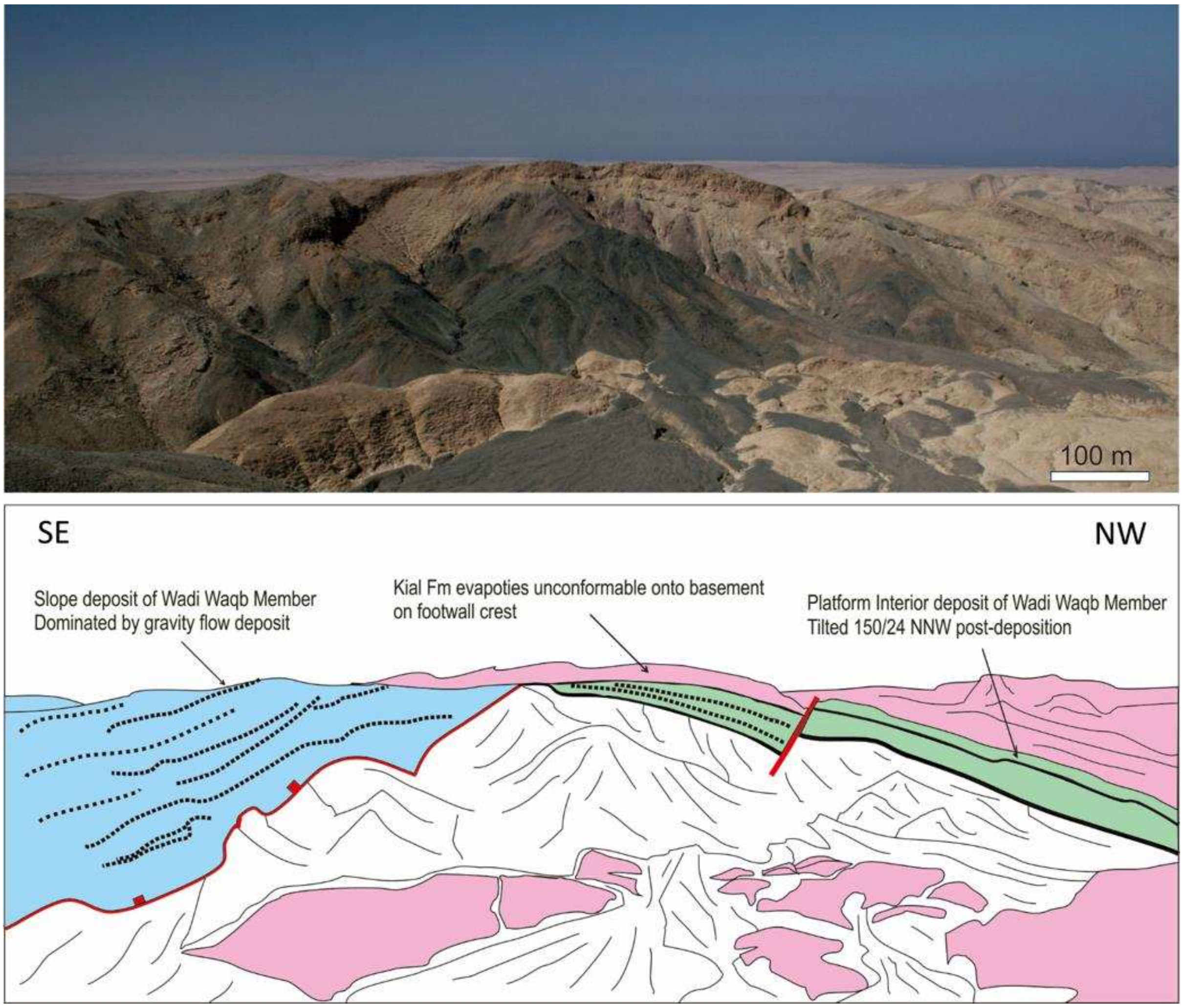
100 m
SE
NW
Slope deposit of Wadi Waqb Member
Dominated by gravity flow deposit
Kial Fm evapoties unconformable onto basement
on footwall crest
Platform Interior deposit of Wadi Waqb Member
Tilted 150/24 NNW post-deposition

Figure. 9

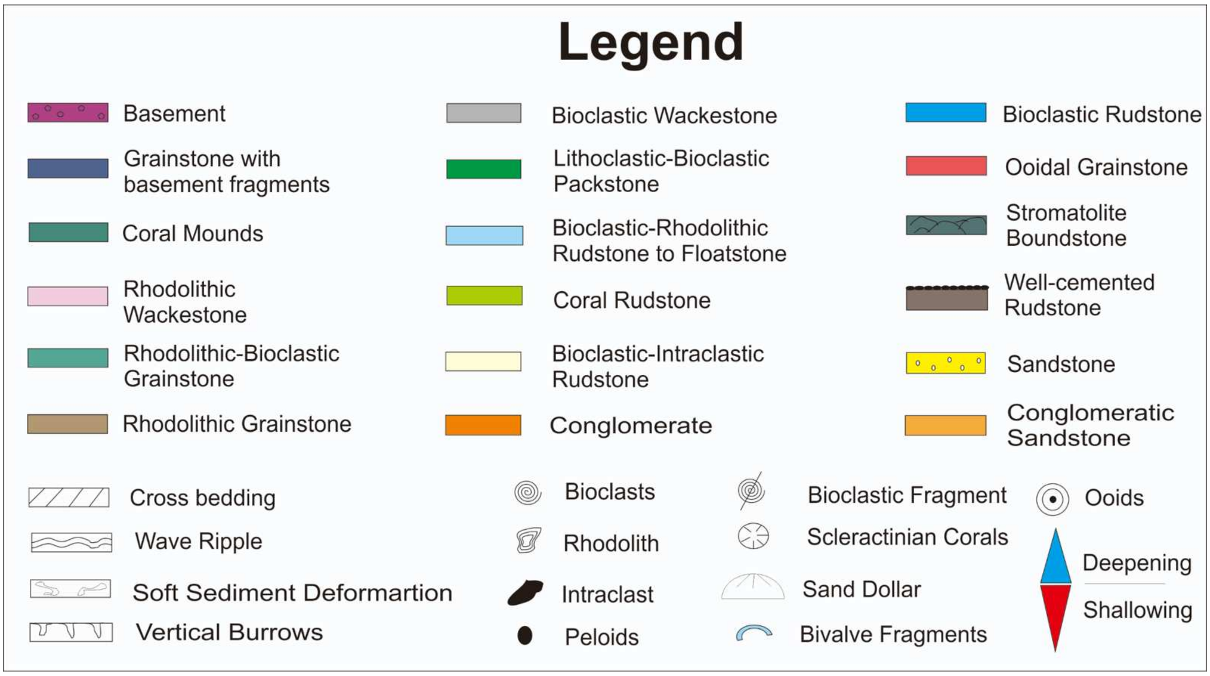
Legend
Basement
Grainstone with basement fragments
Coral Mounds
Rhodolithic Wackestone
Rhodolithic-Bioclastic Grainstone
Rhodolithic Grainstone
Bioclastic Wackestone
Lithoclastic-Bioclastic Packstone
Bioclastic-Rhodolithic Rudstone to Floatstone
Coral Rudstone
Bioclastic-Intraclastic Rudstone
Conglomerate
Bioclastic Rudstone
Ooidal Grainstone
Stromatolite Boundstone
Well-cemented Rudstone
Sandstone
Conglomeratic Sandstone
Cross bedding
Wave Ripple
Soft Sediment Deformartion
Vertical Burrows
Bioclasts
Rhodolith
Intraclast
Peloids
Bioclastic Fragment
Scleractinian Corals
Sand Dollar
Bivalve Fragments
Ooids
Deepening
Shallowing

Figure. 10

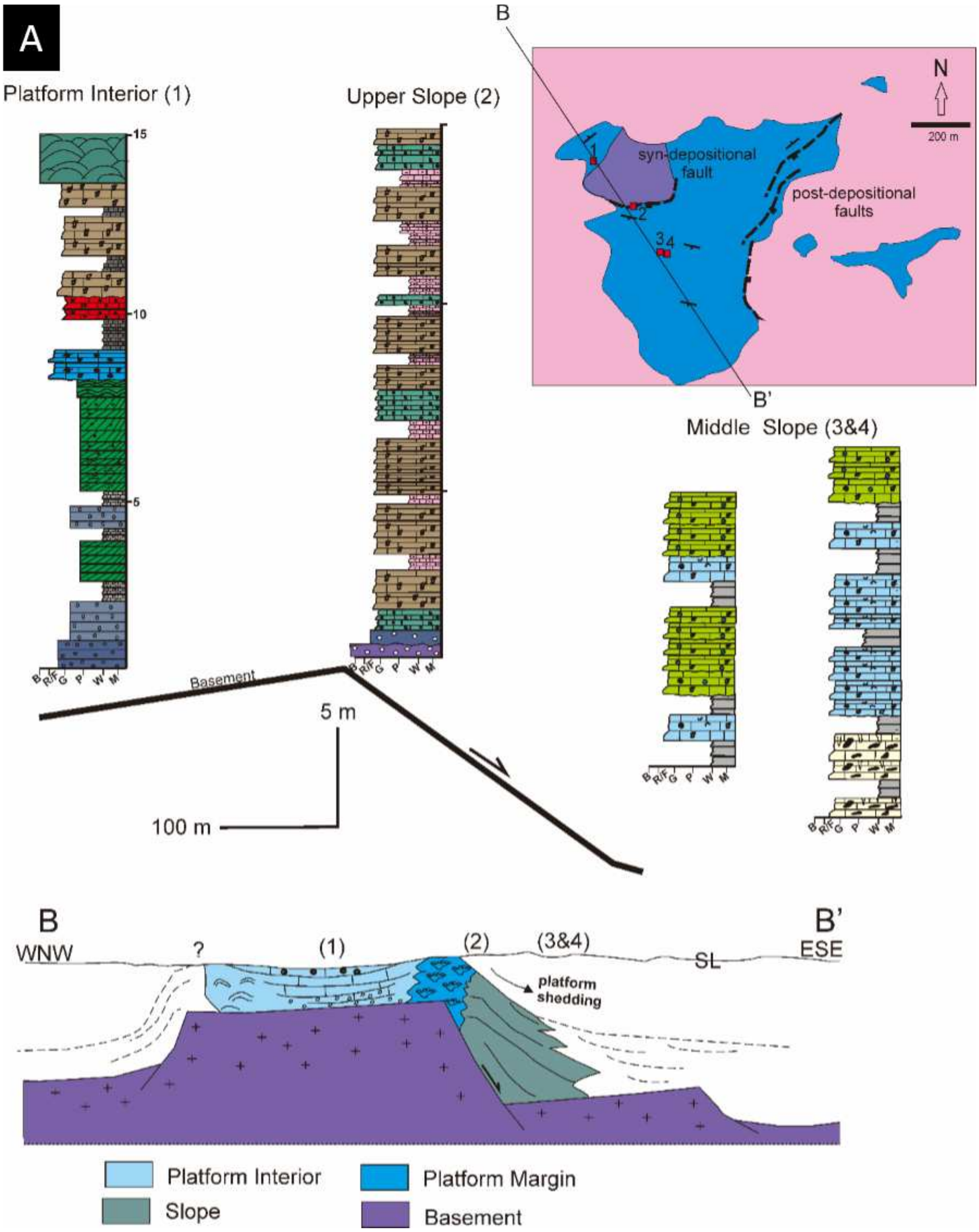
A
Platform Interior (1)
Upper Slope (2)
B
B'
N
200 m
syn-depositional fault
post-depositional faults
Middle Slope (3&4)
B R/F G P W M
Basement
5 m
100 m
B
B'
WNW
ESE
?
(1)
(2)
(3&4)
SL
platform shedding
Platform Interior
Platform Margin
Slope
Basement

Figure. 11A

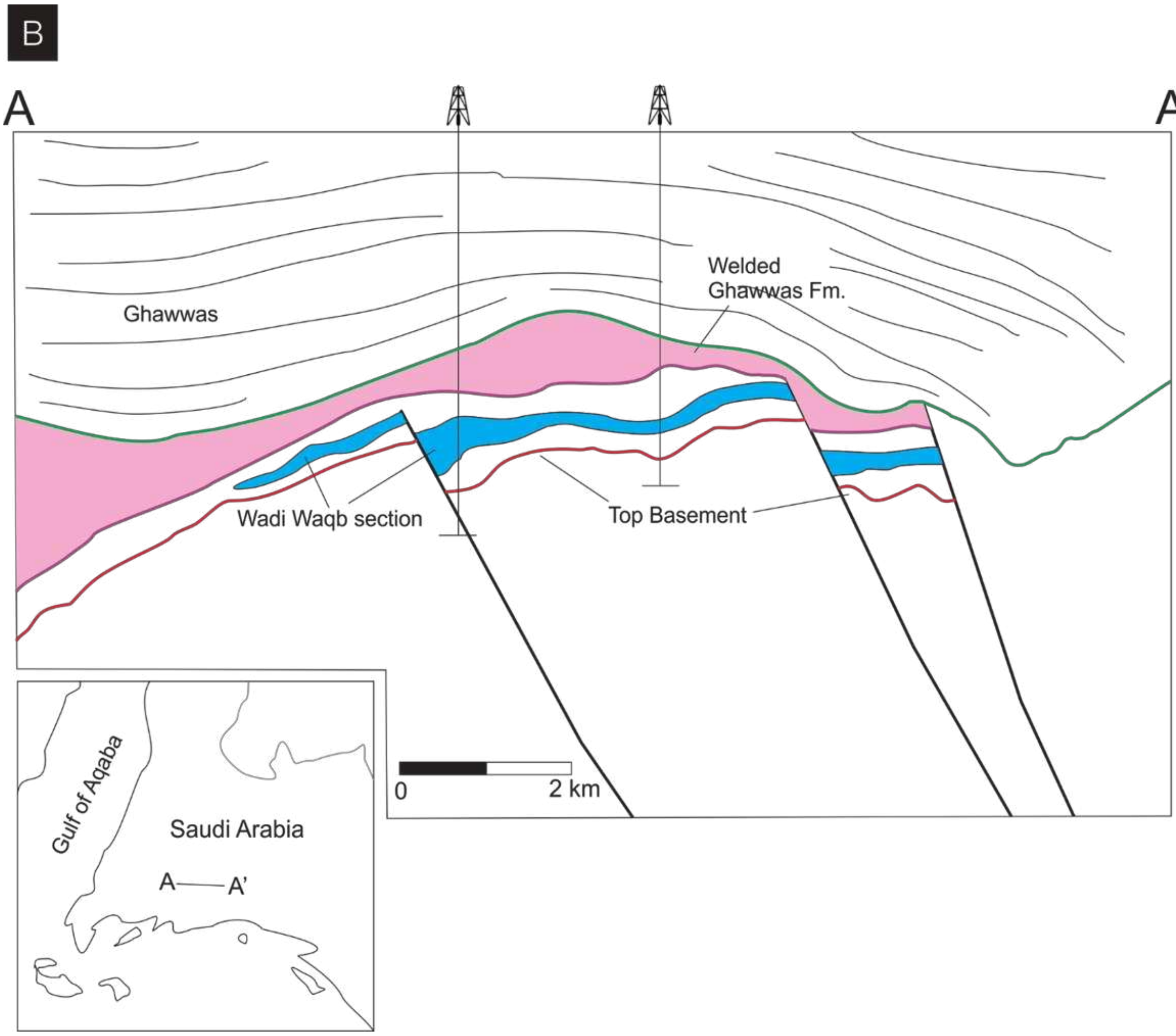
B
A
A'
Welded
Ghawwas Fm.
Ghawwas
Wadi Waqb section
Top Basement
0
2 km
Gulf of Aqaba
Saudi Arabia
A
A'

Figure. 11B

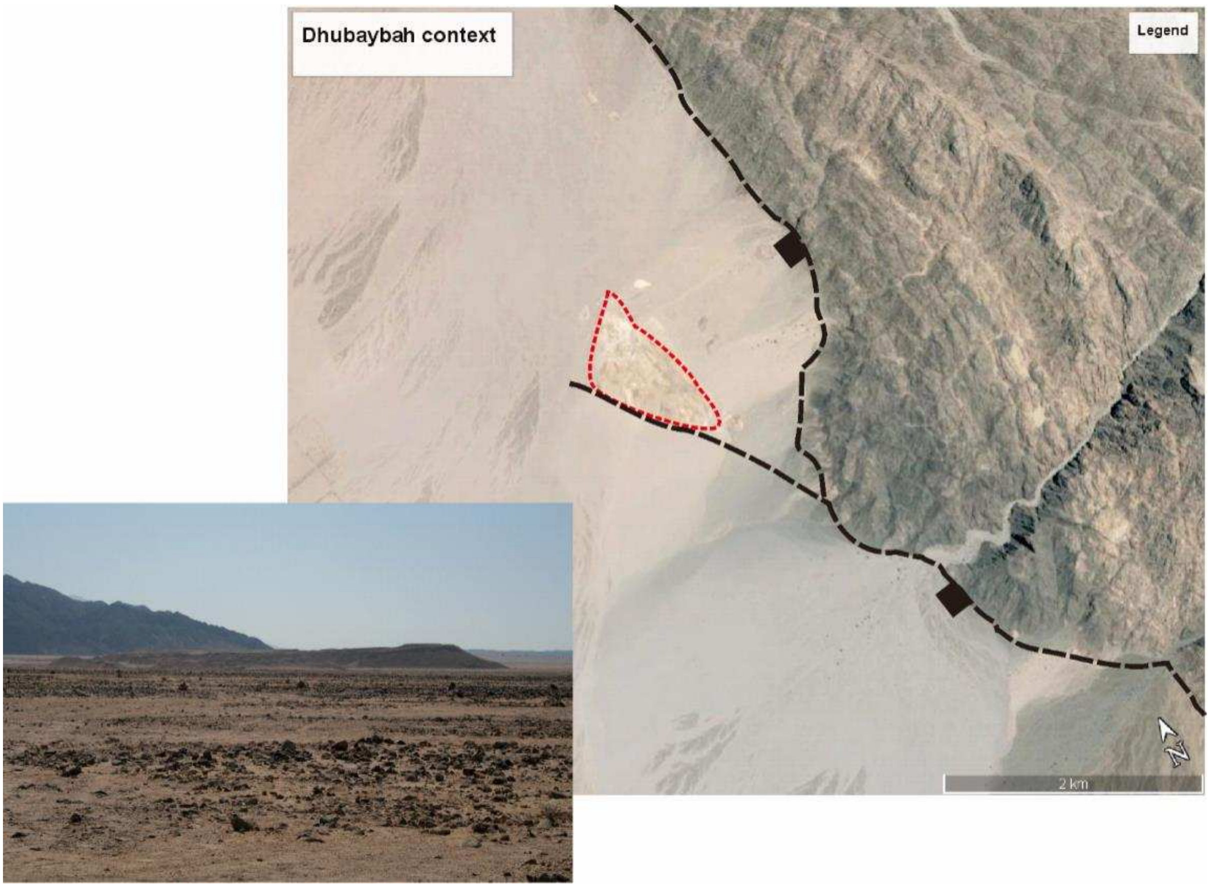

Figure. 12

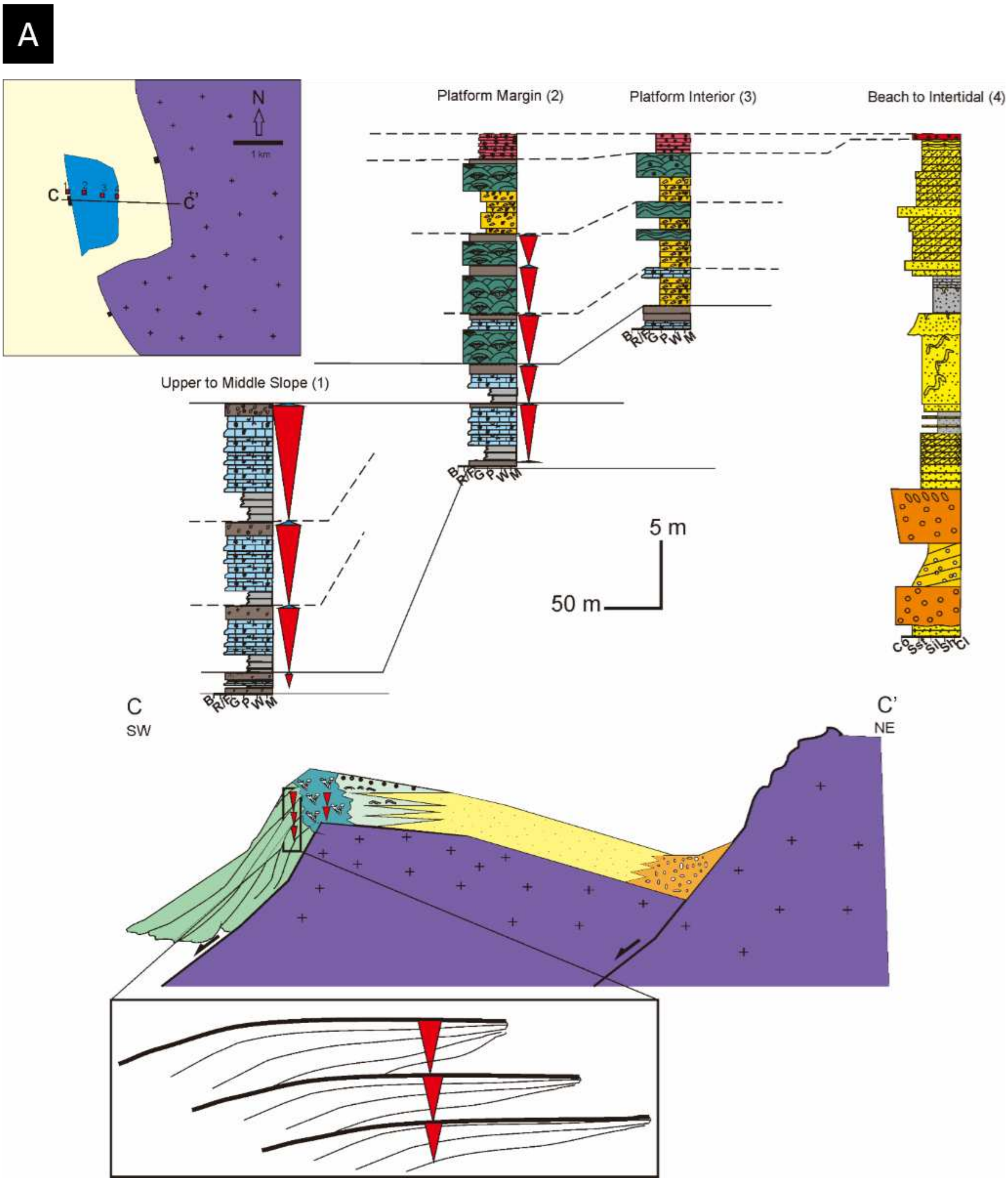
A
N
1 km
C
C'
Platform Margin (2)
Platform Interior (3)
Beach to Intertidal (4)
Upper to Middle Slope (1)
5 m
50 m
C
SW
C'
NE

Figure. 13A

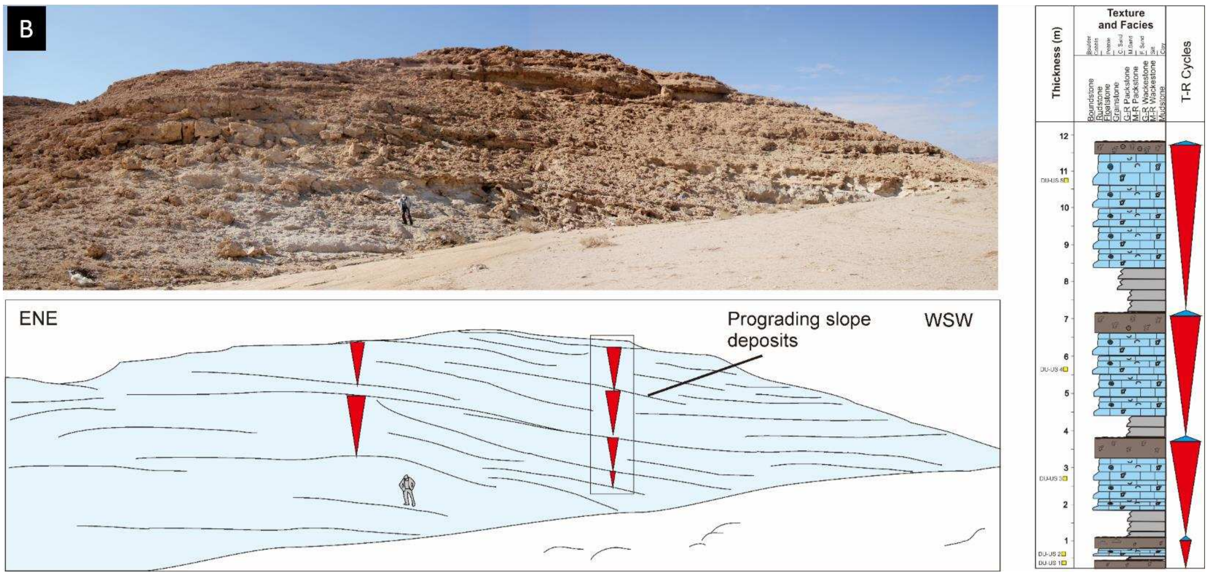
B
ENE
Prograding slope deposits
WSW
Thickness (m)
Texture and Facies
Boundstone
Rudstone
Floatstone
Grainstone
G-R Packstone
M-R Packstone
G-R Wackestone
M-R Wackestone
Mudstone
T-R Cycles
12
11
DU-US 5
10
9
8
7
6
DU-US 4
5
4
3
DU-US 3
2
1
DU-US 2
DU-US 1

Figure. 13B